
A Ranking-based, Balanced Loss Function Unifying Classification and Localisation in Object Detection

Kemal Oksuz, Baris Can Cam, Emre Akbas*, Sinan Kalkan*
 Dept. of Computer Engineering, Middle East Technical University
 Ankara, Turkey
 {kemal.oksuz, can.cam, eakbas, skalkan}@metu.edu.tr

Abstract

We propose *average Localisation-Recall-Precision* (aLRP), a unified, bounded, balanced and ranking-based loss function for both classification and localisation tasks in object detection. aLRP extends the Localisation-Recall-Precision (LRP) performance metric (Oksuz et al., 2018) inspired from how Average Precision (AP) Loss extends precision to a ranking-based loss function for classification (Chen et al., 2020). aLRP has the following distinct advantages: (i) aLRP is the first ranking-based loss function for both classification and localisation tasks. (ii) Thanks to using ranking for both tasks, aLRP naturally enforces high-quality localisation for high-precision classification. (iii) aLRP provides provable balance between positives and negatives. (iv) Compared to on average ~ 6 hyperparameters in the loss functions of state-of-the-art detectors, aLRP Loss has only one hyperparameter, which we did not tune in practice. On the COCO dataset, aLRP Loss improves its ranking-based predecessor, AP Loss, up to around 5 AP points, achieves 48.9 AP without test time augmentation and outperforms all one-stage detectors. Code available at: <https://github.com/kemaloksuz/aLRPLoss>.

1 Introduction

Object detection requires jointly optimizing a classification objective (\mathcal{L}_c) and a localisation objective (\mathcal{L}_r) combined conventionally with a balancing hyperparameter (w_r) as follows:

$$\mathcal{L} = \mathcal{L}_c + w_r \mathcal{L}_r. \quad (1)$$

Optimizing \mathcal{L} in this manner has three critical drawbacks: (D1) It does not correlate the two tasks, and hence, does not guarantee high-quality localisation for high-precision examples (Fig. 1). (D2) It requires a careful tuning of w_r [8, 28, 35], which is prohibitive since a single training may last on the order of days, and ends up with a sub-optimal constant w_r [4, 12]. (D3) It is adversely impeded by the positive-negative imbalance in \mathcal{L}_c and inlier-outlier imbalance in \mathcal{L}_r , thus it requires sampling strategies [14, 15] or specialized loss functions [10, 23], introducing more hyperparameters (Table 1).

A recent solution for D3 is to directly maximize Average Precision (AP) with a loss function called AP Loss [7]. AP Loss is a ranking-based loss function to optimize the ranking of the classification outputs and provides balanced training between positives and negatives.

In this paper, we extend AP Loss to address all three drawbacks (D1-D3) with one, unified loss function called average Localisation Recall Precision (aLRP) Loss. In analogy with the link between precision and AP Loss, we formulate aLRP Loss as the average of LRP values [20] over the positive examples on the Recall-Precision (RP) curve. aLRP has the following benefits: (i) It exploits ranking for both classification and localisation, enforcing high-precision detections to have high-quality

*Equal contribution for senior authorship.

Input Anchors	Classifier Output (C)		Three Possible Localization Outputs					
			Pos. Correlated with C (R_1)		Uncorrelated with C (R_2)		Neg. Correlated with C (R_3)	
	Score	Rank	IoU	Rank	IoU	Rank	IoU	Rank
a ₁	1.00	1	0.95	1	0.80	2	0.50	4
a ₂	0.90	--	--	--	--	--	--	--
a ₃	0.80	2	0.80	2	0.65	3	0.65	3
a ₄	0.70	--	--	--	--	--	--	--
a ₅	0.60	--	--	--	--	--	--	--
a ₆	0.50	3	0.65	3	0.50	4	0.80	2
a ₇	0.40	--	--	--	--	--	--	--
a ₈	0.30	--	--	--	--	--	--	--
a ₉	0.20	--	--	--	--	--	--	--
a ₁₀	0.10	4	0.50	4	0.95	1	0.95	1

(a) 3 possible localization outputs (R_1 - R_3) for the same classifier output (C) (Orange: Positive anchors, Gray: Negative anchors)

Detector Output	AP ₅₀	AP ₆₅	AP ₈₀	AP ₉₅	AP
(C & R_1)	0.51	0.43	0.33	0.20	0.37
(C & R_2)	0.51	0.39	0.24	0.02	0.29
(C & R_3)	0.51	0.19	0.08	0.02	0.20

(b) Performance in AP = (AP₅₀+AP₆₅+AP₈₀+AP₉₅)/4

Detector Output	\mathcal{L}_c		\mathcal{L}_r		Ours
	Cross Entropy	AP Loss	L1 Loss	IoU Loss	aLRP Loss
(C & R_1)	0.87	0.36	0.29	0.28	0.53
(C & R_2)	0.87	0.36	0.29	0.28	0.69
(C & R_3)	0.87	0.36	0.29	0.28	0.89

(c) Comparison of different loss functions (Red: Improper ordering, Green: Proper ordering)

Figure 1: **aLRP Loss enforces high-precision detections to have high-IoUs, while others do not.** (a) Classification and three possible localisation outputs for 10 anchors and the rankings of the positive anchors with respect to (wrt) the scores (for C) and IoUs (for R_1 , R_2 and R_3). Since the regressor is only trained by positive anchors, “--” is assigned for negative anchors. (b,c) Performance and loss assignment comparison of R_1 , R_2 and R_3 when combined with C . When correlation between the rankings of classifier and regressor outputs decreases, performance degrades up to 17 AP (b). While any combination of \mathcal{L}_c and \mathcal{L}_r cannot distinguish them, aLRP Loss penalizes the outputs accordingly (c). The details of the calculations are presented in Appendix A.

Table 1: State-of-the-art loss functions have several hyperparameters (6.4 on avg.). aLRP Loss has only one for step-function approximation (Sec. 2.1). See Appendix B for descriptions of the required hyperparameters. FL: Focal Loss, CE: Cross Entropy, SL1: Smooth L1, H: Hinge Loss.

Method	\mathcal{L}	Number of hyperparameters
AP Loss [7]	AP Loss+ α SL1	3
Focal Loss [15]	FL+ α SL1	4
FCOS [30]	FL+ α IoU+ β CE	4
DR Loss [26]	DR Loss+ α SL1	5
FreeAnchor [35]	$\alpha \log(\max(e^{\text{CE}} \times e^{\beta \text{SL1}})) + \gamma \text{FL}$	8
Faster R-CNN [27]	CE+ α SL1+ β CE+ γ SL1	9
Center Net [8]	FL+FL+ α L2+ β H+ γ (SL1+SL1)	10
Ours	aLRP Loss	1

localisation (Fig. 1). (ii) aLRP has a single hyperparameter (which we did not need to tune) as opposed to ~ 6 in state-of-the-art loss functions (Table 1). (iii) The network is trained by a single loss function that provides provable balance between positives and negatives.

Our contributions are: **(1)** We develop a generalized framework to optimize non-differentiable ranking-based functions by extending the error-driven optimization of AP Loss. **(2)** We prove that ranking-based loss functions conforming to this generalized form provide a natural balance between positive and negative samples. **(3)** We introduce aLRP Loss (and its gradients) as a special case of this generalized formulation. Replacing AP and SmoothL1 losses by aLRP Loss for training RetinaNet improves the performance by up to 5.4AP, and our best model reaches 48.9AP without test time augmentation, outperforming all existing one-stage detectors with significant margin.

1.1 Related Work

Balancing \mathcal{L}_c and \mathcal{L}_r in Eq. (1), an open problem in object detection (OD) [22], bears important challenges: Disposing w_r , and correlating \mathcal{L}_c and \mathcal{L}_r . *Classification-aware regression loss* [3] links the branches by weighing \mathcal{L}_r of an anchor using its classification score. Following Kendall et al.

[12], *LapNet* [4] tackled the challenge by making w_r a learnable parameter based on homoscedastic uncertainty of the tasks. Other approaches [11, 31] combine the outputs of two branches during non-maximum suppression (NMS) at inference. Unlike these methods, aLRP Loss considers the ranking wrt scores for both branches and addresses the imbalance problem naturally.

Ranking-based objectives in OD: An inspiring solution for balancing classes is to optimize a ranking-based objective. However, such objectives are discrete wrt the scores, rendering their direct incorporation challenging. A solution is to use black-box solvers for an interpolated AP loss surface [25], which, however, provided only little gain in performance. AP Loss [7] takes a different approach by using an error-driven update mechanism to calculate gradients (Sec. 2). An alternative, DR Loss [26], employs Hinge Loss to enforce a margin between the scores of the positives and negatives. Despite promising results, these methods are limited to classification and leave localisation as it is. In contrast, we propose a single, balanced, ranking-based loss to train both branches.

2 Background

2.1 AP Loss and Error-Driven Optimization

AP Loss [7] directly optimizes the following loss for AP with intersection-over-union (IoU) thresholded at 0.50:

$$\mathcal{L}^{\text{AP}} = 1 - \text{AP}_{50} = 1 - \frac{1}{|\mathcal{P}|} \sum_{i \in \mathcal{P}} \text{precision}(i) = 1 - \frac{1}{|\mathcal{P}|} \sum_{i \in \mathcal{P}} \frac{\text{rank}^+(i)}{\text{rank}(i)}, \quad (2)$$

where \mathcal{P} is the set of positives; $\text{rank}^+(i)$ and $\text{rank}(i)$ are respectively the ranking positions of the i th sample among positives and all samples. $\text{rank}(i)$ can be easily defined using a step function $H(\cdot)$ applied on the difference between the score of i (s_i) and the score of each other sample:

$$\text{rank}(i) = 1 + \sum_{j \in \mathcal{P}, j \neq i} H(x_{ij}) + \sum_{j \in \mathcal{N}} H(x_{ij}), \quad (3)$$

where $x_{ij} = -(s_i - s_j)$ is positive if $s_i < s_j$; \mathcal{N} is the set of negatives; and $H(x) = 1$ if $x \geq 0$ and $H(x) = 0$ otherwise. In practice, $H(\cdot)$ is replaced by $x/2\delta + 0.5$ in the interval $[-\delta, \delta]$ (in aLRP, we use $\delta = 1$ as set by AP Loss [7] empirically; this is the only hyperparameter of aLRP – Table 1). $\text{rank}^+(i)$ can be defined similarly over $j \in \mathcal{P}$. With this notation, \mathcal{L}^{AP} can be rewritten as follows:

$$\mathcal{L}^{\text{AP}} = \frac{1}{|\mathcal{P}|} \sum_{i \in \mathcal{P}} \sum_{j \in \mathcal{N}} \frac{H(x_{ij})}{\text{rank}(i)} = \frac{1}{|\mathcal{P}|} \sum_{i \in \mathcal{P}} \sum_{j \in \mathcal{N}} L_{ij}^{\text{AP}}, \quad (4)$$

where L_{ij}^{AP} is called a *primary term* which is zero if $i \notin \mathcal{P}$ or $j \notin \mathcal{N}$.

Note that this system is composed of two parts: (i) The differentiable part up to x_{ij} , and (ii) the non-differentiable part that follows x_{ij} . Chen et al. proposed that an error-driven update of x_{ij} (inspired from perceptron learning [29]) can be combined with derivatives of the differentiable part. Consider the update in x_{ij} that minimizes L_{ij}^{AP} (and hence \mathcal{L}^{AP}): $\Delta x_{ij} = L_{ij}^{\text{AP}*} - L_{ij}^{\text{AP}} = 0 - L_{ij}^{\text{AP}} = -L_{ij}^{\text{AP}}$, with the target, $L_{ij}^{\text{AP}*}$, being zero for perfect ranking. Chen et al. showed that the gradient of L_{ij}^{AP} wrt x_{ij} can be taken as $-\Delta x_{ij}$. With this, the gradient of \mathcal{L}^{AP} wrt scores can be calculated as follows:

$$\frac{\partial \mathcal{L}^{\text{AP}}}{\partial s_i} = \sum_{j,k} \frac{\partial \mathcal{L}^{\text{AP}}}{\partial x_{jk}} \frac{\partial x_{jk}}{\partial s_i} = -\frac{1}{|\mathcal{P}|} \sum_{j,k} \Delta x_{jk} \frac{\partial x_{jk}}{\partial s_i} = \frac{1}{|\mathcal{P}|} \left(\sum_j \Delta x_{ij} - \sum_j \Delta x_{ji} \right). \quad (5)$$

2.2 Localisation-Recall-Precision (LRP) Performance Metric

LRP [20, 21] is a metric that quantifies classification and localisation performances jointly. Given a detection set thresholded at a score (s) and their matchings with the ground truths, LRP aims to assign an error value within $[0, 1]$ by considering localisation, recall and precision:

$$\text{LRP}(s) = \frac{1}{N_{FP} + N_{FN} + N_{TP}} \left(N_{FP} + N_{FN} + \sum_{k \in TP} \mathcal{E}_{loc}(k) \right), \quad (6)$$

²By setting $L_{ij}^{\text{AP}} = 0$ when $i \notin \mathcal{P}$ or $j \notin \mathcal{N}$, we do not require the y_{ij} term used by Chen et al. [7].

where N_{FP} , N_{FN} and N_{TP} are the number of false positives (FP), false negatives (FN) and true positives (TP); A detection is a TP if $\text{IoU}(k) \geq \tau$ where $\tau = 0.50$ is the conventional TP labeling threshold, and a TP has a localisation error of $\mathcal{E}_{loc}(k) = (1 - \text{IoU}(k))/(1 - \tau)$. The detection performance is, then, $\min_s(\text{LRP}(s))$ on the precision-recall (PR) curve, called optimal LRP (oLRP).

3 A Generalisation of Error-Driven Optimization for Ranking-Based Losses

Generalizing the error-driven optimization technique of AP Loss [7] to other ranking-based loss functions is not trivial. In particular, identifying the primary terms is a challenge especially when the loss has components that involve only positive examples, such as the localisation error in aLRP Loss.

Given a ranking-based loss function, $\mathcal{L} = \frac{1}{Z} \sum_{i \in \mathcal{P}} \ell(i)$, defined as a sum over individual losses, $\ell(i)$, at positive examples (e.g., Eq. (2)), with Z as a problem specific normalization constant, our goal is to express \mathcal{L} as a sum of *primary terms* in a more general form than Eq. (4):

Definition 1. The *primary term* L_{ij} concerning examples $i \in \mathcal{P}$ and $j \in \mathcal{N}$ is the loss originating from i and distributed over j via a probability mass function $p(j|i)$. Formally,

$$L_{ij} = \begin{cases} \ell(i)p(j|i), & \text{for } i \in \mathcal{P}, j \in \mathcal{N} \\ 0, & \text{otherwise.} \end{cases} \quad (7)$$

Then, as desired, we can express $\mathcal{L} = \frac{1}{Z} \sum_{i \in \mathcal{P}} \ell(i)$ in terms of L_{ij} :

Theorem 1. $\mathcal{L} = \frac{1}{Z} \sum_{i \in \mathcal{P}} \ell(i) = \frac{1}{Z} \sum_{i \in \mathcal{P}} \sum_{j \in \mathcal{N}} L_{ij}$. See Appendix C for the proof.

Eq. (7) makes it easier to define primary terms and adds more flexibility on the error distribution: e.g., AP Loss takes $p(j|i) = H(x_{ij})/N_{FP}(i)$, which distributes error uniformly (since it is reduced to $1/N_{FP}(i)$) over $j \in \mathcal{N}$ with $s_j \geq s_i$; though, a skewed $p(j|i)$ can be used to promote harder examples (i.e. larger x_{ij}). Here, $N_{FP}(i) = \sum_{j \in \mathcal{N}} H(x_{ij})$ is the number of false positives for $i \in \mathcal{P}$.

Now we can identify the gradients of this generalized definition following Chen et al. (Sec. 2.1): The error-driven update in x_{ij} that would minimize \mathcal{L} is $\Delta x_{ij} = L_{ij}^* - L_{ij}$, where L_{ij}^* denotes ‘‘the primary term when i is ranked properly’’. Note that L_{ij}^* , which is set to zero in AP Loss, needs to be carefully defined (see Appendix G for a bad example). With Δx_{ij} defined, the gradients can be derived similar to Eq. (5). The steps for obtaining the gradients of \mathcal{L} are summarized in Algorithm 1.

Algorithm 1 Obtaining the gradients of a ranking-based function with error-driven update.

Input: A ranking-based function $\mathcal{L} = (\ell(i), Z)$, and a probability mass function $p(j|i)$

Output: The gradient of \mathcal{L} with respect to model output \mathbf{s}

- 1: $\forall i, j$ find primary term: $L_{ij} = \ell(i)p(j|i)$ if $i \in \mathcal{P}, j \in \mathcal{N}$; otherwise $L_{ij} = 0$ (c.f. Eq. (7)).
 - 2: $\forall i, j$ find target primary term: $L_{ij}^* = \ell(i)^*p(j|i)$ ($\ell(i)^*$: the error on i when i is ranked properly.)
 - 3: $\forall i, j$ find error-driven update: $\Delta x_{ij} = L_{ij}^* - L_{ij} = (\ell(i)^* - \ell(i)) p(j|i)$.
 - 4: **return** $\frac{1}{Z} (\sum_j \Delta x_{ij} - \sum_j \Delta x_{ji})$ for each $s_i \in \mathbf{s}$ (c.f. Eq. (5)).
-

This optimization provides balanced training for ranking-based losses conforming to Theorem 1:

Theorem 2. Training is balanced between positive and negative examples at each iteration; i.e. the summed gradient magnitudes of positives and negatives are equal (see Appendix C for the proof):

$$\sum_{i \in \mathcal{P}} \left| \frac{\partial \mathcal{L}}{\partial s_i} \right| = \sum_{i \in \mathcal{N}} \left| \frac{\partial \mathcal{L}}{\partial s_i} \right|. \quad (8)$$

Deriving AP Loss. Let us derive AP Loss as a case example for this generalized framework: $\ell^{\text{AP}}(i)$ is simply $1 - \text{precision}(i) = N_{FP}(i)/\text{rank}(i)$, and $Z = |\mathcal{P}|$. $p(j|i)$ is assumed to be uniform, i.e. $p(j|i) = H(x_{ij})/N_{FP}(i)$. These give us $L_{ij}^{\text{AP}} = \frac{N_{FP}(i)}{\text{rank}(i)} \frac{H(x_{ij})}{N_{FP}(i)} = \frac{H(x_{ij})}{\text{rank}(i)}$ (c.f. L_{ij}^{AP} in Eq. (4)). Then, since $L_{ij}^{\text{AP}*} = 0$, $\Delta x_{ij} = 0 - L_{ij}^{\text{AP}} = -L_{ij}^{\text{AP}}$ in Eq. (5).

Deriving Normalized Discounted Cumulative Gain Loss [18]: See Appendix D.

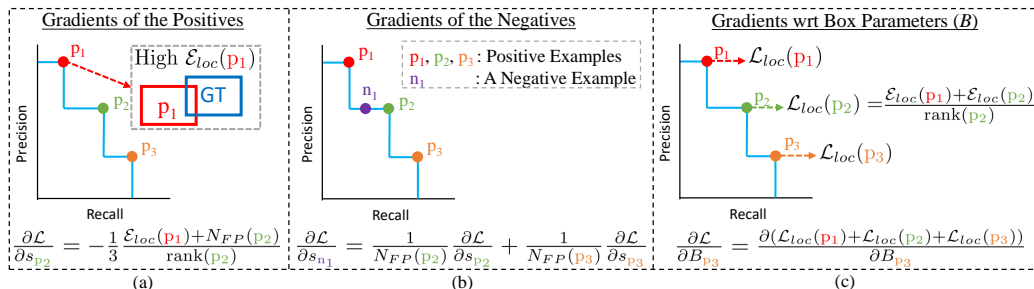


Figure 2: **aLRP Loss assigns gradients to each branch based on the outputs of both branches.** Examples on the PR curve are in sorted order wrt scores (s). \mathcal{L} refers to $\mathcal{L}^{\text{aLRP}}$. **(a)** A p_i 's gradient wrt its score considers (i) localisation errors of examples with larger s (e.g. high $\mathcal{E}_{loc}(p_1)$ increases the gradient of s_{p_2} to suppress p_1), (ii) number of negatives with larger s . **(b)** Gradients wrt s of the negatives: The gradient of a p_i is uniformly distributed over the negatives with larger s . Summed contributions from all positives determine the gradient of a negative. **(c)** Gradients of the box parameters: While p_1 (with highest s) is included in total localisation error on each positive, i.e. $\mathcal{L}_{loc}(i) = \frac{1}{\text{rank}(i)} (\mathcal{E}_{loc}(i) + \sum_{k \in \mathcal{P}, k \neq i} \mathcal{E}_{loc}(k) H(x_{ik}))$, p_3 is included once with the largest rank(p_i).

4 Average Localisation-Recall-Precision (aLRP) Loss

Similar to the relation between precision and AP Loss, aLRP Loss is defined as the average of LRP values ($\ell^{\text{LRP}}(i)$) of positive examples:

$$\mathcal{L}^{\text{aLRP}} := \frac{1}{|\mathcal{P}|} \sum_{i \in \mathcal{P}} \ell^{\text{LRP}}(i). \quad (9)$$

For LRP, we assume that anchors are dense enough to cover all ground-truths, i.e. $N_{FN} = 0$. Also, since a detection is enforced to follow the label of its anchor during training, TP and FP sets are replaced by the thresholded subsets of \mathcal{P} and \mathcal{N} , respectively. This is applied by $H(\cdot)$, and $\text{rank}(i) = N_{TP} + N_{FP}$ from Eq. (6). Then, following the definitions in Sec. 2.1, $\ell^{\text{LRP}}(i)$ is:

$$\ell^{\text{LRP}}(i) = \frac{1}{\text{rank}(i)} \left(N_{FP}(i) + \mathcal{E}_{loc}(i) + \sum_{k \in \mathcal{P}, k \neq i} \mathcal{E}_{loc}(k) H(x_{ik}) \right). \quad (10)$$

Note that Eq. (10) allows using robust forms of IoU-based losses (e.g. generalized IoU (GIoU) [28]) only by replacing IoU Loss (i.e. $1 - \text{IoU}(i)$) in $\mathcal{E}_{loc}(i)$ and normalizing the range to $[0, 1]$.

In order to provide more insight and facilitate gradient derivation, we split Eq. (9) into two as localisation and classification components such that $\mathcal{L}^{\text{aLRP}} = \mathcal{L}_{cls}^{\text{aLRP}} + \mathcal{L}_{loc}^{\text{aLRP}}$, where

$$\mathcal{L}_{cls}^{\text{aLRP}} = \frac{1}{|\mathcal{P}|} \sum_{i \in \mathcal{P}} \frac{N_{FP}(i)}{\text{rank}(i)}, \text{ and } \mathcal{L}_{loc}^{\text{aLRP}} = \frac{1}{|\mathcal{P}|} \sum_{i \in \mathcal{P}} \frac{1}{\text{rank}(i)} \left(\mathcal{E}_{loc}(i) + \sum_{k \in \mathcal{P}, k \neq i} \mathcal{E}_{loc}(k) H(x_{ik}) \right). \quad (11)$$

4.1 Optimization of the aLRP Loss

$\mathcal{L}^{\text{aLRP}}$ is differentiable wrt the estimated box parameters, B , since \mathcal{E}_{loc} is differentiable [28, 32] (i.e. the derivatives of $\mathcal{L}_{cls}^{\text{aLRP}}$ and $\text{rank}(\cdot)$ wrt B are 0). However, $\mathcal{L}_{cls}^{\text{aLRP}}$ and $\mathcal{L}_{loc}^{\text{aLRP}}$ are not differentiable wrt the classification scores, and therefore, we need the generalized framework from Sec. 3.

Using the same error distribution from AP Loss, the primary terms of aLRP Loss can be defined as $L_{ij}^{\text{aLRP}} = \ell^{\text{LRP}}(i)p(j|i)$. As for the target primary terms, we use the following desired LRP Error:

$$\ell^{\text{LRP}}(i)^* = \frac{1}{\text{rank}(i)} \left(\overset{0}{N_{FP}(i)} + \mathcal{E}_{loc}(i) + \sum_{k \in \mathcal{P}, k \neq i} \mathcal{E}_{loc}(k) H(x_{ik}) \right) \overset{0}{=} \frac{\mathcal{E}_{loc}(i)}{\text{rank}(i)}, \quad (12)$$

yielding a target primary term, $L_{ij}^{\text{aLRP}*} = \ell^{\text{LRP}}(i)^* p(j|i)$, which includes localisation error and can be non-zero when $s_i < s_j$, unlike AP Loss. Then, the resulting error-driven update for x_{ij} is (line 3 of Algorithm 1):

$$\Delta x_{ij} = \left(\ell^{\text{LRP}}(i)^* - \ell^{\text{LRP}}(i) \right) p(j|i) = -\frac{1}{\text{rank}(i)} \left(N_{FP}(i) + \sum_{k \in \mathcal{P}, k \neq i} \mathcal{E}_{loc}(k) H(x_{ik}) \right) \frac{H(x_{ij})}{N_{FP}(i)}. \quad (13)$$

Finally, $\partial \mathcal{L}^{\text{aLRP}} / \partial s_i$ can be obtained with Eq. (5). Our algorithm to compute the loss and gradients is presented in Appendix E in detail and has the same time&space complexity with AP Loss.

Interpretation of the Components: A distinctive property of aLRP Loss is that classification and localisation errors are handled in a unified manner: i.e. with aLRP, both classification and localisation branches use the entire output of the detector, instead of working in their separate domains as conventionally done. As shown in Fig. 2(a,b), $\mathcal{L}_{cls}^{\text{aLRP}}$ takes into account localisation errors of detections with larger scores (s) and promotes the detections with larger IoUs to have higher s , or suppresses the detections with high- s &low-IoU. Similarly, $\mathcal{L}_{loc}^{\text{aLRP}}$ inherently weighs each positive based on its classification rank (see Appendix F for the weights): the contribution of a positive increases if it has a larger s . To illustrate, in Fig. 2(c), while $\mathcal{E}_{loc}(p_1)$ (i.e. with largest s) contributes to each $\mathcal{L}_{loc}(i)$; $\mathcal{E}_{loc}(p_3)$ (i.e. with the smallest s) only contributes once with a very low weight due to its rank normalizing $\mathcal{L}_{loc}(p_3)$. Hence, the localisation branch effectively focuses on detections ranked higher wrt s .

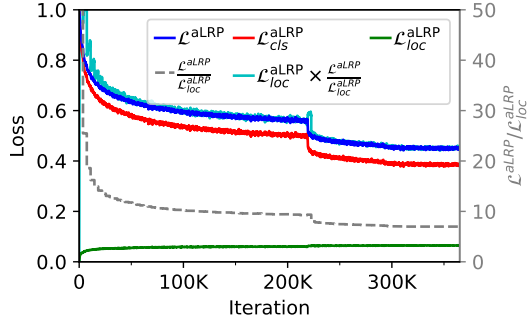


Figure 3: aLRP Loss and its components. The localisation component is self-balanced.

4.2 A Self-Balancing Extension for the Localisation Task

LRP metric yields localisation error only if a detection is classified correctly (Sec. 2.2). Hence, when the classification performance is poor (e.g. especially at the beginning of training), the aLRP Loss is dominated by the classification error ($N_{FP}(i)/\text{rank}(i) \approx 1$ and $\ell^{\text{LRP}}(i) \in [0, 1]$ in Eq. (10)). As a result, the localisation head is hardly trained at the beginning (Fig. 3). Moreover, Fig. 3 also shows that $\mathcal{L}_{cls}^{\text{aLRP}} / \mathcal{L}_{loc}^{\text{aLRP}}$ varies significantly throughout training. To alleviate this, we propose a simple and dynamic *self-balancing* (SB) strategy using the gradient magnitudes: note that $\sum_{i \in \mathcal{P}} \left| \partial \mathcal{L}^{\text{aLRP}} / \partial s_i \right| = \sum_{i \in \mathcal{N}} \left| \partial \mathcal{L}^{\text{aLRP}} / \partial s_i \right| \approx \mathcal{L}^{\text{aLRP}}$ (see Theorem 2 and Appendix F). Then, assuming that the gradients wrt scores and boxes are proportional to their contributions to the aLRP Loss, we multiply $\partial \mathcal{L}^{\text{aLRP}} / \partial B$ by the average $\mathcal{L}^{\text{aLRP}} / \mathcal{L}_{loc}^{\text{aLRP}}$ of the previous epoch.

5 Experiments

Dataset: We train all our models on COCO *trainval35K* set [16] (115K images), test on *minival* set (5k images) and compare with the state-of-the-art (SOTA) on *test-dev* set (20K images).

Performance Measures: COCO-style AP [16] and when possible optimal LRP [20] (Sec. 2.2) are used for comparison. For more insight into aLRP Loss, we use Pearson correlation coefficient (ρ) to measure correlation between the rankings of classification and localisation, averaged over classes.

Implementation Details: For training, we use 4 v100 GPUs. The batch size is 32 for training with 512×512 images (aLRPLoss500), whereas it is 16 for 800×800 images (aLRPLoss800). Following AP Loss, our models are trained for 100 epochs using stochastic gradient descent with a momentum factor of 0.9. We use a learning rate of 0.008 for aLRPLoss500 and 0.004 for aLRPLoss800, each decreased by factor 0.1 at epochs 60 and 80. Similar to previous work [7, 8], standard data augmentation methods from SSD [17] are used. At test time, we rescale shorter sides of images to

Table 2: Ablation analysis on COCO *minival*. For optimal LRP (oLRP), lower is better.

Method	Rank-Based \mathcal{L}_c	Rank-Based \mathcal{L}_r	SB	ATSS	AP	AP ₅₀	AP ₇₅	AP ₉₀	oLRP	ρ
AP Loss [7]	✓				35.5	58.0	37.0	9.0	71.0	0.45
aLRP Loss	✓	✓(w IoU)			36.9	57.7	38.4	13.9	69.9	0.49
	✓	✓(w IoU)	✓		38.7	58.1	40.6	17.4	68.5	0.48
	✓	✓(w GIoU)	✓		38.9	58.5	40.5	17.4	68.4	0.48
	✓	✓(w GIoU)	✓	✓	40.2	60.3	42.3	18.1	67.3	0.48

Table 3: SB does not require tuning and slightly outperforms constant weighting for both IoU types.

w_r	1	2	5	10	15	20	25	SB
w IoU	36.9	37.8	38.5	38.6	38.3	37.1	36.0	38.7
w GIoU	36.0	37.0	37.9	38.7	38.8	38.7	38.8	38.9

Table 4: SB is not affected significantly by the initial weight in the first epoch (w_r) even for large values.

w_r	1	50	100	500
AP	38.8	38.9	38.7	38.5

500 (aLRPLoss500) or 800 (aLRPLoss800) pixels by ensuring that the longer side does not exceed $1.66\times$ of the shorter side. NMS is applied to 1000 top-scoring detections using 0.50 as IoU threshold.

5.1 Ablation Study

In this section, in order to provide a fair comparison, we build upon the official implementation of our baseline, AP Loss [5]. Keeping all design choices fixed, otherwise stated, we just replace AP & Smooth L1 losses by aLRP Loss to optimize RetinaNet [15]. We conduct ablation analysis using aLRPLoss500 on ResNet-50 backbone (more ablation experiments are presented in the Appendix G).

Effect of using ranking for localisation: Table 2 shows that using a ranking loss for localisation improves AP (from 35.5 to 36.9). For better insight, AP₉₀ is also included in Table 2, which shows ~ 5 points increase despite similar AP₅₀ values. This confirms that aLRP Loss does produce high-quality outputs for both branches, and boosts the performance for larger IoUs.

Effect of Self-Balancing (SB): Section 4.2 and Fig. 3 discussed how \mathcal{L}_{cls}^{aLRP} and \mathcal{L}_{loc}^{aLRP} behave during training and introduced self-balancing to improve training of the localisation branch. Table 2 shows that SB provides +1.8AP gain, similar AP₅₀ and +8.4 points in AP₉₀ against AP Loss. Comparing SB with constant weighting in Table 3, our SB approach provides slightly better performance than constant weighting, which requires extensive tuning and end up with different w_r constants for IoU and GIoU. Finally, Table 4 presents that initialization of SB (i.e. its value for the first epoch) has a negligible effect on the performance even with very large values. We use 50 for initialization.

Using GIoU: Table 2 suggests robust IoU-based regression (GIoU) improves performance slightly.

Using ATSS: Finally, we replace the standard IoU-based assignment by ATSS [34], which uses less anchors and decreases training time notably for aLRP Loss: One iteration drops from 0.80s to 0.53s with ATSS (34% more efficient with ATSS) – this time is 0.71s and 0.28s for AP Loss and Focal Loss respectively. With ATSS, we also observe +1.3AP improvement (Table 2). See App. G for details.

Hence, we use GIoU [28] as part of aLRP Loss, and employ ATSS [34] when training RetinaNet.

5.2 More insight on aLRP Loss

Potential of Correlating Classification and Localisation.

We analyze two bounds: (i) A *Lower Bound* where localisation provides an inverse ranking compared to classification. (ii) An *Upper Bound* where localisation provides exactly the same ranking as classification. Table 5 shows that correlating ranking can have a significant effect (up to 20 AP) on the performance especially for larger IoUs. Therefore, correlating rankings promises significant improvement (up to ~ 10 AP). Moreover, while ρ is 0.44 and 0.45 for Focal Loss (results not provided in the table) and AP Loss (Table 2), respectively, aLRP Loss yields higher correlation (0.48, 0.49).

Table 5: Effect of correlating rankings.

\mathcal{L}	ρ	AP	AP ₅₀	AP ₇₅	AP ₉₀
aLRP Loss	0.48	38.7	58.1	40.6	17.4
Lower Bound	-1.00	28.6	58.1	23.6	5.6
Upper Bound	1.00	48.1	58.1	51.9	33.9

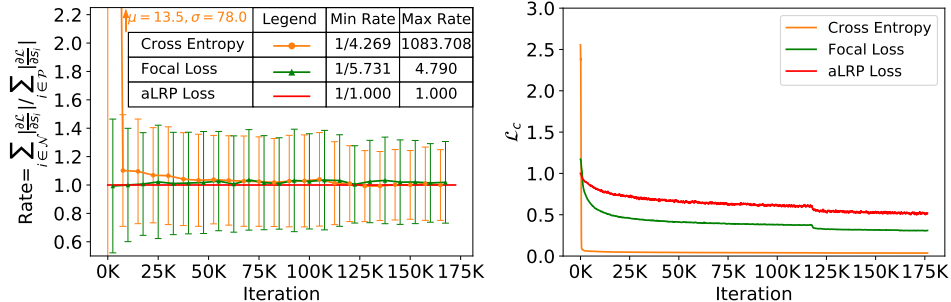


Figure 4: **(left)** The rate of the total gradient magnitudes of negatives to positives. **(right)** Loss values.

Analysing Balance Between Positives and Negatives. For this analysis, we compare Cross Entropy Loss (CE), Focal Loss (FL) and aLRP Loss on RetinaNet trained for 12 epochs and average results over 10 runs. Fig. 4 experimentally confirms Theorem 2 for aLRP Loss (\mathcal{L}_{cls}^{aLRP}), as it exhibits perfect balance between the gradients throughout training. However, we see large fluctuations in derivatives of CE and FL (left), which biases training towards positives or negatives alternately across iterations. As expected, imbalance impacts CE more as it quickly drops (right), overfitting in favor of negatives since it is dominated by the error and gradients of these large amount of negatives.

5.3 Comparison with State of the Art (SOTA)

Different from the ablation analysis, we find it useful to decrease the learning rate of aLRPLoss500 at epochs 75 and 95. For SOTA comparison, we use the mmdetection framework [6] for efficiency (we reproduced Table 2 using our mmdetection implementation, yielding similar results - see our repository). Table 6 presents the results, which are discussed below:

Ranking-based Losses. aLRP Loss yields significant gains over other ranking-based solutions: e.g., compared with AP Loss, aLRP Loss provides +5.4AP for scale 500 and +5.1AP for scale 800. Similarly, for scale 800, aLRP Loss performs 4.7AP better than DR Loss with ResNeXt-101.

Methods combining branches. Although a direct comparison is not fair since different conditions are used, we observe a significant margin (around 3-5AP in scale 800) compared to other approaches that combine localisation and classification.

Comparison on scale 500. We see that, even with ResNet-101, aLRPLoss500 outperforms all other methods with 500 test scale. With ResNext-101, aLRP Loss outperforms its closest counterpart (HSD) by 2.7AP and also in all sizes ($AP_S - AP_L$).

Comparison on scale 800. For 800 scale, aLRP Loss achieves 45.9 and 47.8AP on ResNet-101 and ResNeXt-101 backbones respectively. Also in this scale, aLRP Loss consistently outperforms its closest counterparts (i.e. FreeAnchor and CenterNet) by 2.9AP and reaches the highest results wrt all performance measures. With DCN [37], aLRP Loss reaches 48.9AP, outperforming ATSS by 1.2AP.

5.4 Using aLRP Loss with Different Object Detectors

Here, we use aLRP Loss to train FoveaBox [13] as an anchor-free detector, and Faster R-CNN [27] as a two-stage detector. All models use 500 scale setting, have a ResNet-50 backbone and follow our mmdetection implementation [6]. Further implementation details are presented in Appendix G.

Results on FoveaBox: To train FoveaBox, we keep the learning rate same with RetinaNet (i.e. 0.008) and only replace the loss function by aLRP Loss. Table 7 shows that aLRP Loss outperforms Focal Loss and AP Loss, each combined by Smooth L1 (SL1 in Table 7), by 1.4 and 3.2 AP points (and similar oLRP points) respectively. Note that aLRP Loss also simplifies tuning hyperparameters of Focal Loss, which are set in FoveaBox to different values from RetinaNet. One training iteration of Focal Loss, AP Loss and aLRP Loss take 0.34, 0.47 and 0.54 sec respectively.

Results on Faster R-CNN: To train Faster R-CNN, we remove sampling, use aLRP Loss to train both stages (i.e. RPN and Fast R-CNN) and reweigh aLRP Loss of RPN by 0.20. Thus, the number

Table 6: Comparison with the SOTA detectors on COCO *test-dev*. $S, \times 1.66$ implies that the image is rescaled such that its longer side cannot exceed $1.66 \times S$ where S is the size of the shorter side. R:ResNet, X:ResNeXt, H:HourglassNet, D:DarkNet, De:DeNet. We use ResNeXt101 64x4d.

Method	Backbone	Training Size	Test Size	AP	AP ₅₀	AP ₇₅	AP _S	AP _M	AP _L
<i>One-Stage Methods</i>									
RefineDet [33] [‡]	R-101	512 × 512	512 × 512	36.4	57.5	39.5	16.6	39.9	51.4
EFGRNet [19] [‡]	R-101	512 × 512	512 × 512	39.0	58.8	42.3	17.8	43.6	54.5
ExtremeNet [36] ^{*‡}	H-104	511 × 511	original	40.2	55.5	43.2	20.4	43.2	53.1
RetinaNet [15]	X-101	800, × 1.66	800, × 1.66	40.8	61.1	44.1	24.1	44.2	51.2
HSD [2] [‡]	X-101	512 × 512	512 × 512	41.9	61.1	46.2	21.8	46.6	57.0
FCOS [30] [†]	X-101	(640, 800), × 1.66	800, × 1.66	44.7	64.1	48.4	27.6	47.5	55.6
CenterNet [8] ^{*‡}	H-104	511 × 511	original	44.9	62.4	48.1	25.6	47.4	57.4
ATSS [34] [†]	X-101-DCN	(640, 800), × 1.66	800, × 1.66	47.7	66.5	51.9	29.7	50.8	59.4
<i>Ranking Losses</i>									
AP Loss500 [7] [‡]	R-101	512 × 512	500, × 1.66	37.4	58.6	40.5	17.3	40.8	51.9
AP Loss800 [7] [‡]	R-101	800 × 800	800, × 1.66	40.8	63.7	43.7	25.4	43.9	50.6
DR Loss [26] [†]	X-101	(640, 800), × 1.66	800, × 1.66	43.1	62.8	46.4	25.6	46.2	54.0
<i>Combining Branches</i>									
LapNet [4]	D-53	512 × 512	512 × 512	37.6	55.5	40.4	17.6	40.5	49.9
Fitness NMS [31]	De-101	512, × 1.66	768, × 1.66	39.5	58.0	42.6	18.9	43.5	54.1
Retina+PISA [3]	R-101	800, × 1.66	800, × 1.66	40.8	60.5	44.2	23.0	44.2	51.4
FreeAnchor [35] [†]	X-101	(640, 800), × 1.66	800, × 1.66	44.9	64.3	48.5	26.8	48.3	55.9
<i>Ours</i>									
aLRP Loss500 [‡]	R-50	512 × 512	500, × 1.66	41.3	61.5	43.7	21.9	44.2	54.0
aLRP Loss500 [‡]	R-101	512 × 512	500, × 1.66	42.8	62.9	45.5	22.4	46.2	56.8
aLRP Loss500 [‡]	X-101	512 × 512	500, × 1.66	44.6	65.0	47.5	24.6	48.1	58.3
aLRP Loss800 [‡]	R-101	800 × 800	800, × 1.66	45.9	66.4	49.1	28.5	48.9	56.7
aLRP Loss800 [‡]	X-101	800 × 800	800, × 1.66	47.8	68.4	51.1	30.2	50.8	59.1
aLRP Loss800 [‡]	X-101-DCN	800 × 800	800, × 1.66	48.9	69.3	52.5	30.8	51.5	62.1
<i>Multi-Scale Test</i>									
aLRP Loss800 [‡]	X-101-DCN	800 × 800	800, × 1.66	50.2	70.3	53.9	32.0	53.1	63.0

[†]: multiscale training, [‡]: SSD-like augmentation, *: Soft NMS [1] and flip augmentation at test time

Table 7: Comparison on FoveaBox [13].

\mathcal{L}	AP	AP ₅₀	AP ₇₅	AP ₉₀	oLRP
Focal Loss+SLI	38.3	57.8	40.7	15.7	68.8
AP Loss+SLI	36.5	58.3	38.2	11.3	69.8
aLRP Loss (Ours)	39.7	58.8	41.5	18.2	67.2

Table 8: Comparison on Faster R-CNN [27]

\mathcal{L}	AP	AP ₅₀	AP ₇₅	AP ₉₀	oLRP
Cross Entropy+L1	37.8	58.1	41.0	12.2	69.3
Cross Entropy+GIoU	38.2	58.2	41.3	13.7	69.0
aLRP Loss (Ours)	40.7	60.7	43.3	18.0	66.7

of hyperparameters is reduced from nine (Table 1) to three (two δ s for step function, and a weight for RPN). We validated the learning rate of aLRP Loss as 0.012, and train baseline Faster R-CNN by both L1 Loss and GIoU Loss for fair comparison. aLRP Loss outperforms these baselines by more than 2.5AP and 2oLRP points while simplifying the training pipeline (Table 8). One training iteration of Cross Entropy Loss (with L1) and aLRP Loss take 0.38 and 0.85 sec respectively.

6 Conclusion

In this paper, we provided a general framework for the error-driven optimization of ranking-based functions. As a special case of this generalization, we introduced aLRP Loss, a ranking-based, balanced loss function which handles the classification and localisation errors in a unified manner. aLRP Loss has only one hyperparameter which we did not need to tune, as opposed to around 6 in SOTA loss functions. We showed that using aLRP improves its baselines significantly over different detectors by simplifying parameter tuning, and outperforms all one-stage detectors.

Broader Impact

We anticipate our work to significantly impact the following domains:

1. **Object detection:** Our loss function is unique in many important aspects: It unifies localisation and classification in a single loss function. It uses ranking for both classification and localisation. It provides provable balance between negatives and positives, similar to AP Loss.
These unique merits will contribute to a paradigm shift in the object detection community towards more capable and sophisticated loss functions such as ours.
2. **Other computer vision problems with multiple objectives:** Problems including multiple objectives (such as instance segmentation, panoptic segmentation – which actually has classification and regression objectives) will benefit significantly from our proposal of using ranking for both classification and localisation.
3. **Problems that can benefit from ranking:** Many vision problems can be easily converted into a ranking problem. They can then exploit our generalized framework to easily define a loss function and to determine the derivatives.

Our paper does not have direct social implications. However, it inherits the following implications of object detectors: Object detectors can be used for surveillance purposes for the betterness of society albeit privacy concerns. When used for detecting targets, an object detector’s failure may have severe consequences depending on the application (e.g. self-driving cars). Moreover, such detectors are affected by the bias in data, although they will not try to exploit them for any purposes.

Acknowledgments and Disclosure of Funding

This work was partially supported by the Scientific and Technological Research Council of Turkey (TÜBİTAK) through a project titled “Object Detection in Videos with Deep Neural Networks” (grant number 117E054). Kemal Öksüz is supported by the TÜBİTAK 2211-A National Scholarship Programme for Ph.D. students. The numerical calculations reported in this paper were performed at TUBITAK ULAKBIM High Performance and Grid Computing Center (TRUBA), and Roketsan Missiles Inc. sources.

References

- [1] Bodla N, Singh B, Chellappa R, Davis LS (2017) Soft-nms – improving object detection with one line of code. In: The IEEE International Conference on Computer Vision (ICCV)
- [2] Cao J, Pang Y, Han J, Li X (2019) Hierarchical shot detector. In: The IEEE International Conference on Computer Vision (ICCV)
- [3] Cao Y, Chen K, Loy CC, Lin D (2019) Prime Sample Attention in Object Detection. arXiv 1904.04821
- [4] Chabot F, Pham QC, Chaouch M (2019) Lapnet : Automatic balanced loss and optimal assignment for real-time dense object detection. arXiv 1911.01149
- [5] Chen K (Last Accessed: 14 May 2020) Ap-loss. <https://github.com/cccorn/AP-loss>
- [6] Chen K, Wang J, Pang J, Cao Y, Xiong Y, Li X, Sun S, Feng W, Liu Z, Xu J, Zhang Z, Cheng D, Zhu C, Cheng T, Zhao Q, Li B, Lu X, Zhu R, Wu Y, Dai J, Wang J, Shi J, Ouyang W, Loy CC, Lin D (2019) MMDetection: Open mmlab detection toolbox and benchmark. arXiv 1906.07155
- [7] Chen K, Lin W, j li, See J, Wang J, Zou J (2020) Ap-loss for accurate one-stage object detection. IEEE Transactions on Pattern Analysis and Machine Intelligence pp 1–1
- [8] Duan K, Bai S, Xie L, Qi H, Huang Q, Tian Q (2019) Centernet: Keypoint triplets for object detection. In: The IEEE International Conference on Computer Vision (ICCV)

- [9] Everingham M, Van Gool L, Williams CKI, Winn J, Zisserman A (2010) The pascal visual object classes (voc) challenge. *International Journal of Computer Vision (IJCV)* 88(2):303–338
- [10] Girshick R (2015) Fast R-CNN. In: *The IEEE International Conference on Computer Vision (ICCV)*
- [11] Jiang B, Luo R, Mao J, Xiao T, Jiang Y (2018) Acquisition of localization confidence for accurate object detection. In: *The European Conference on Computer Vision (ECCV)*
- [12] Kendall A, Gal Y, Cipolla R (2018) Multi-task learning using uncertainty to weigh losses for scene geometry and semantics. In: *The IEEE Conference on Computer Vision and Pattern Recognition (CVPR)*
- [13] Kong T, Sun F, Liu H, Jiang Y, Li L, Shi J (2020) Foveabox: Beyond anchor-based object detection. *IEEE Transactions on Image Processing* 29:7389–7398
- [14] Li B, Liu Y, Wang X (2019) Gradient harmonized single-stage detector. In: *AAAI Conference on Artificial Intelligence*
- [15] Lin T, Goyal P, Girshick R, He K, Dollár P (2020) Focal loss for dense object detection. *IEEE Transactions on Pattern Analysis and Machine Intelligence* 42(2):318–327
- [16] Lin TY, Maire M, Belongie S, Hays J, Perona P, Ramanan D, Dollár P, Zitnick CL (2014) Microsoft COCO: Common Objects in Context. In: *The European Conference on Computer Vision (ECCV)*
- [17] Liu W, Anguelov D, Erhan D, Szegedy C, Reed SE, Fu C, Berg AC (2016) SSD: single shot multibox detector. In: *The European Conference on Computer Vision (ECCV)*
- [18] Mohapatra P, Rolínek M, Jawahar C, Kolmogorov V, Pawan Kumar M (2018) Efficient optimization for rank-based loss functions. In: *The IEEE Conference on Computer Vision and Pattern Recognition (CVPR)*
- [19] Nie J, Anwer RM, Cholakkal H, Khan FS, Pang Y, Shao L (2019) Enriched feature guided refinement network for object detection. In: *The IEEE International Conference on Computer Vision (ICCV)*
- [20] Oksuz K, Cam BC, Akbas E, Kalkan S (2018) Localization recall precision (LRP): A new performance metric for object detection. In: *The European Conference on Computer Vision (ECCV)*
- [21] Oksuz K, Cam BC, Akbas E, Kalkan S (2020) One metric to measure them all: Localisation recall precision (lrp) for evaluating visual detection tasks. *arXiv* 2011.10772
- [22] Oksuz K, Cam BC, Kalkan S, Akbas E (2020) Imbalance problems in object detection: A review. *IEEE Transactions on Pattern Analysis and Machine Intelligence (TPAMI)* pp 1–1
- [23] Pang J, Chen K, Shi J, Feng H, Ouyang W, Lin D (2019) Libra R-CNN: Towards balanced learning for object detection. In: *The IEEE Conference on Computer Vision and Pattern Recognition (CVPR)*
- [24] Peng C, Xiao T, Li Z, Jiang Y, Zhang X, Jia K, Yu G, Sun J (2018) Megdet: A large mini-batch object detector. In: *The IEEE Conference on Computer Vision and Pattern Recognition (CVPR)*
- [25] Pogančić MV, Paulus A, Musil V, Martius G, Rolínek M (2020) Differentiation of blackbox combinatorial solvers. In: *International Conference on Learning Representations (ICLR)*
- [26] Qian Q, Chen L, Li H, Jin R (2020) Dr loss: Improving object detection by distributional ranking. In: *The IEEE Conference on Computer Vision and Pattern Recognition (CVPR)*
- [27] Ren S, He K, Girshick R, Sun J (2017) Faster R-CNN: Towards real-time object detection with region proposal networks. *IEEE Transactions on Pattern Analysis and Machine Intelligence* 39(6):1137–1149

- [28] Rezatofighi H, Tsoi N, Gwak J, Sadeghian A, Reid I, Savarese S (2019) Generalized intersection over union: A metric and a loss for bounding box regression. In: The IEEE Conference on Computer Vision and Pattern Recognition (CVPR)
- [29] Rosenblatt F (1958) The perceptron: A probabilistic model for information storage and organization in the brain. *Psychological Review* pp 65–386
- [30] Tian Z, Shen C, Chen H, He T (2019) Fcos: Fully convolutional one-stage object detection. In: The IEEE International Conference on Computer Vision (ICCV)
- [31] Tychsens-Smith L, Petersson L (2018) Improving object localization with fitness nms and bounded iou loss. In: The IEEE Conference on Computer Vision and Pattern Recognition (CVPR)
- [32] Yu J, Jiang Y, Wang Z, Cao Z, Huang T (2016) Unitbox: An advanced object detection network. In: The ACM International Conference on Multimedia
- [33] Zhang S, Wen L, Bian X, Lei Z, Li SZ (2018) Single-shot refinement neural network for object detection. In: The IEEE Conference on Computer Vision and Pattern Recognition (CVPR)
- [34] Zhang S, Chi C, Yao Y, Lei Z, Li SZ (2020) Bridging the gap between anchor-based and anchor-free detection via adaptive training sample selection. In: IEEE/CVF Conference on Computer Vision and Pattern Recognition (CVPR)
- [35] Zhang X, Wan F, Liu C, Ji R, Ye Q (2019) Freeanchor: Learning to match anchors for visual object detection. In: *Advances in Neural Information Processing Systems (NeurIPS)*
- [36] Zhou X, Zhuo J, Krahenbuhl P (2019) Bottom-up object detection by grouping extreme and center points. In: The IEEE Conference on Computer Vision and Pattern Recognition (CVPR)
- [37] Zhu X, Hu H, Lin S, Dai J (2019) Deformable convnets v2: More deformable, better results. In: IEEE/CVF Conference on Computer Vision and Pattern Recognition (CVPR)

APPENDIX

A Details of Figure 1: Comparison of Loss Functions on a Toy Example

This section aims to present the scenario considered in Figure 1 of the main paper. Section A.1 explains the scenario, Section A.2 and Section A.3 clarify how the performance measures (AP, AP_{50} , etc.) and loss values (cross-entropy, AP Loss, aLRP Loss, etc.) are calculated.

A.1 The Scenario

We assume that the scenario in Figure 1(a) of the paper includes five ground truths of which four of them are detected as true positives with different Intersection-over-Union (IoU) overlaps by three different detectors (i.e. $C\&R_1$, $C\&R_2$, $C\&R_3$). Each detector has a different ranking for these true positives with respect to their IoUs. In addition, the output of each detector contains the same six detections with different scores as false positives. Note that the IoUs of these false positives are marked with "-" in Figure 1(a) since they do not match with any ground truth and therefore their IoUs are not being considered neither by the performance measure (i.e. Average Precision) nor by loss computation.

A.2 Performance Evaluation

There are different ways to calculate Average Precision (AP) and loss values. For example, in PASCAL [9] and COCO [16] datasets, the recall domain is divided into 11 and 101 evenly spaced points, respectively, and the precision values at these points are averaged to compute AP for a single IoU threshold.

Here, we present how Average Precision (AP) is calculated in Figure 1(b). Similar to the widely adopted performance metric, COCO-style AP, we use AP_{IoU} with different IoU thresholds. In order

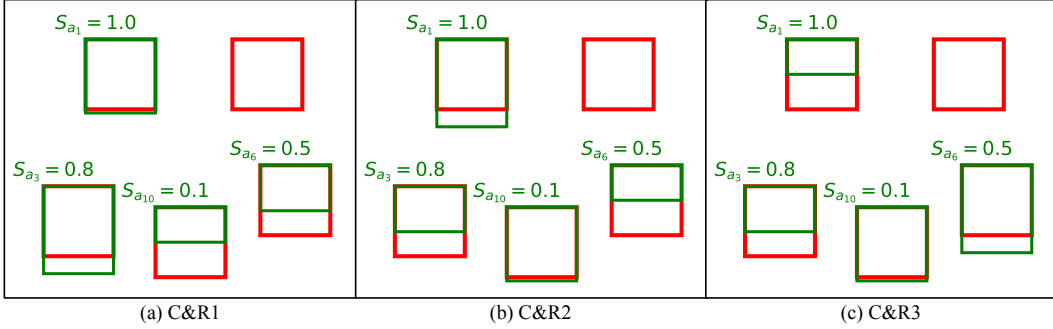


Figure A.5: Visualization of anchor boxes in the scenarios used in Figure 1. Green and red boxes are positive anchors and ground truths respectively. p_i refers to confidence score of the anchor a_i . Note that for all of the scenarios, there are additionally six false positives (see Figure 1), which are excluded in this figure for clarity.

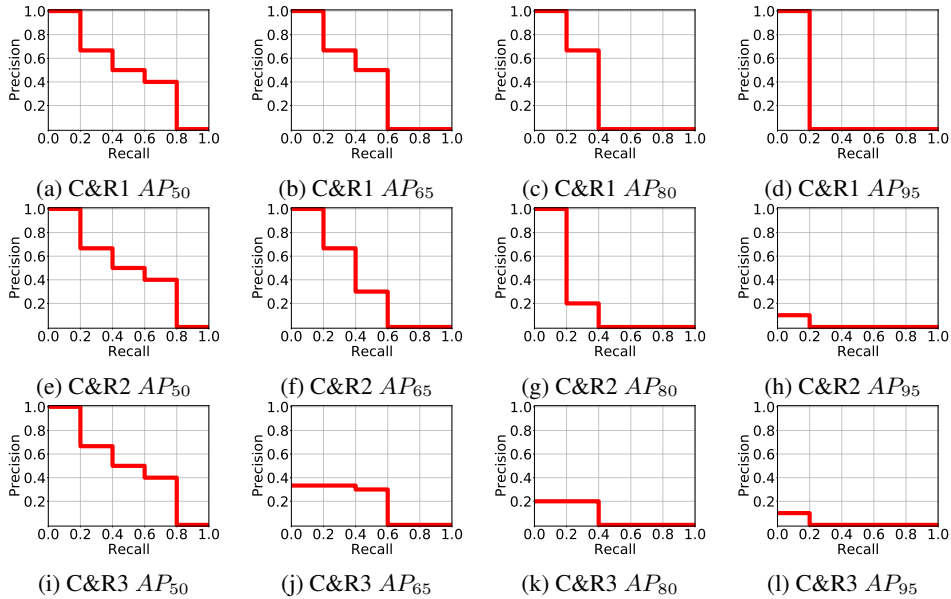


Figure A.6: PR curve of each detector output- AP_{IoU} pair. Rows and columns correspond to different AP_{IoU} and detector outputs respectively. PR curves are interpolated (see the text for more detail).

to keep things simple but provide the essence of the performance metric, we use four samples with 0.15 increments (i.e. $\{0.50, 0.65, 0.80, 0.95\}$) instead of ten samples with 0.05 increments as done by original COCO-style AP.

In order to compute a single average precision with an IoU as the conventional true positive labelling threshold, denoted by AP_{IoU} , the approaches use different methods for sampling/combining individual precision values on a PR curve. The PR curves corresponding to each detector- AP_{IoU} pair are presented in Figure A.6. While drawing these curves, similar to Pascal-VOC and COCO, we also adopt interpolation on the PR curve, which requires keeping the larger precision value in the case that the larger one resides in a lower recall. Then, again similar to what these common methods do for a single AP threshold, we check the precision values on different recall values after splitting the recall axis equally. Here, we use 10 recall points between 0.1 and 1.0 in 0.1 increments. Then, based on the PR curves in Figure A.6, we check the precision under these different recall values and present them in Table A.9. Having generated these values in Table A.9 for each AP_{IoU} s, the computation is trivial: Just averaging over these precisions (i.e. row-wise average) yields AP_{IoU} s. Finally, averaging over these four AP_{IoU} s produces the final detection performance as 0.37, 0.29 and 0.20 for C&R₁, C&R₂, C&R₃ respectively (see Table A.9).

Table A.9: Precision of each detector output-AP_{IoU} pair for evenly spaced recall values. This table is based on the PR curves presented in Fig. A.6.

IoU	Output	Precisions for Different Recalls (R)										AP _{IoU}
		R=0.1	R=0.2	R=0.3	R=0.4	R=0.5	R=0.6	R=0.7	R=0.8	R=0.9	R=1.0	
0.50	C&R ₁	1.00	1.00	0.67	0.67	0.50	0.50	0.40	0.40	0.00	0.00	0.51
	C&R ₂	1.00	1.00	0.67	0.67	0.50	0.50	0.40	0.40	0.00	0.00	0.51
	C&R ₃	1.00	1.00	0.67	0.67	0.50	0.50	0.40	0.40	0.00	0.00	0.51
0.65	C&R ₁	1.00	1.00	0.67	0.67	0.50	0.50	0.00	0.00	0.00	0.00	0.43
	C&R ₂	1.00	1.00	0.67	0.67	0.30	0.30	0.00	0.00	0.00	0.00	0.39
	C&R ₃	0.33	0.33	0.33	0.33	0.30	0.30	0.00	0.00	0.00	0.00	0.19
0.80	C&R ₁	1.00	1.00	0.67	0.67	0.00	0.00	0.00	0.00	0.00	0.00	0.33
	C&R ₂	1.00	1.00	0.20	0.20	0.00	0.00	0.00	0.00	0.00	0.00	0.24
	C&R ₃	0.20	0.20	0.20	0.20	0.00	0.00	0.00	0.00	0.00	0.00	0.08
0.95	C&R ₁	1.00	1.00	0.00	0.00	0.00	0.00	0.00	0.00	0.00	0.00	0.20
	C&R ₂	0.10	0.10	0.00	0.00	0.00	0.00	0.00	0.00	0.00	0.00	0.02
	C&R ₃	0.10	0.10	0.00	0.00	0.00	0.00	0.00	0.00	0.00	0.00	0.02

A.3 Computing the Loss Values

In this section, computing the loss values in Figure 1(c) of the paper is presented in detail. Each section is devoted to a loss function presented in Figure 1(c). To keep things simple, without loss of generality, we make the following assumptions in this section during the calculation of the classification and localisation losses:

1. The classifier has sigmoid non-linearity at the top.
2. There is only one foreground class.
3. Similar to how localisation losses deal with scale- and translation-variance within an image, we assume that each ground truth box is normalized as $[0, 0, 1, 1]$.
4. For each loss, the average of its contributors is reported.

A.3.1 Cross-entropy Loss

Cross-entropy Loss of the i th example is defined as:

$$\mathcal{L}^{CE}(p_i) = -\mathcal{I}[i \in \mathcal{P}] \log(p_i) - \mathcal{I}[i \in \mathcal{N}] \log(1 - p_i), \quad (\text{A.14})$$

such that p_i is the confidence score of the i th example obtained by applying the sigmoid activation to the classification logit s_i , and $\mathcal{I}[Q]$ is the Iverson bracket which is 1 if the predicate Q is true; or else it is 0.

Seeing that all detector outputs, $C\&R_1$, $C\&R_2$ and $C\&R_3$, involve the same classification output, we apply Eq. (A.14) for each anchor on C , and then find their average as follows:

$$\mathcal{L}^{CE} = \frac{1}{|\mathcal{P}| + |\mathcal{N}|} \sum_{p_i} \mathcal{L}^{CE}(p_i), \quad (\text{A.15})$$

$$= -\frac{1}{10} (\log(1.00) + \log(1 - 0.90) + \log(0.80) + \log(1 - 0.70) + \log(1 - 0.60) + \log(0.50) \quad (\text{A.16})$$

$$+ \log(1 - 0.40) + \log(1 - 0.30) + \log(1 - 0.20) + \log(0.10)), \quad (\text{A.17})$$

$$= 0.87. \quad (\text{A.18})$$

A.3.2 Average precision (AP) Loss

The computation of AP Loss is very similar to the AP₅₀ computation described in Section A.2 except that precision is calculated on (and also averaged over) the positive examples instead of the recall values. With this intuition the precision values on the four positives are 1.00, 0.67, 0.50, 0.40

respectively. Then, AP Loss for the output C in Figure 1 regardless of the localisation output that it is combined with is:

$$\begin{aligned}\mathcal{L}^{AP} &= 1 - \text{AP}_{50} = 1 - \frac{1}{|\mathcal{P}|} \sum_{i \in \mathcal{P}} \text{precision}(i), \\ &= 1 - \frac{1}{4} \times (1.00 + 0.67 + 0.50 + 0.40) = 0.36.\end{aligned}$$

A.3.3 L1 Loss

For a single ground truth, $\hat{B}_i = [\hat{x}_1, \hat{y}_1, \hat{x}_2, \hat{y}_2]$, and its corresponding detection, $B_i = [x_1, y_1, x_2, y_2]$, L1 Loss is defined simply by averaging over the L1 norm of the differences of the parameters of the detection boxes from their corresponding ground truths:

$$\mathcal{L}^{L1}(\hat{B}_i, B_i) = |\hat{x}_1 - x_1| + |\hat{y}_1 - y_1| + |\hat{x}_2 - x_2| + |\hat{y}_2 - y_2|, \quad (\text{A.19})$$

Then, the average L1 Loss is:

$$\mathcal{L}^{L1} = \frac{1}{|\mathcal{P}|} \sum_{i \in \mathcal{P}} \mathcal{L}^{L1}(\hat{B}_i, B_i), \quad (\text{A.20})$$

$$= \frac{1}{4} \left((0.00 + 0.00 + 0.00 + 0.05) + (0.00 + 0.00 + 0.00 + 0.25) \right) \quad (\text{A.21})$$

$$+ (0.00 + 0.00 + 0.00 + 0.35) + (0.00 + 0.00 + 0.00 + 0.50) \Big), \quad (\text{A.22})$$

$$= 0.29. \quad (\text{A.23})$$

A.3.4 IoU Loss

For a single example, IoU Loss is simply $1 - \text{IoU}(\hat{B}_i, B_i)$. Then, for all three outputs in the scenario (also an instance is illustrated in Figure A.5), seeing that the IoU distributions are all equal, the average IoU loss of this detection set is:

$$\begin{aligned}\mathcal{L}^{\text{IoU}} &= \frac{1}{|\mathcal{P}|} \sum_{i \in \mathcal{P}} 1 - \text{IoU}(\hat{B}_i, B_i), \\ &= \frac{1}{4} \left((1 - 0.95) + (1 - 0.80) + (1 - 0.65) + (1 - 0.50) \right) = 0.28.\end{aligned}$$

A.3.5 aLRP Loss

This section calculates aLRP Loss value in the scenario, and therefore we believe that at the same time it is also a toy example to present more insight on aLRP Loss.

First, let us recall the definition of aLRP Loss from the paper to simplify tracking this section. aLRP Loss is defined as:

$$\mathcal{L}^{\text{aLRP}} := \frac{1}{|\mathcal{P}|} \sum_{i \in \mathcal{P}} \ell^{\text{LRP}}(i), \quad (\text{A.24})$$

such that

$$\ell^{\text{LRP}}(i) = \frac{1}{\text{rank}(i)} \left(N_{FP}(i) + \mathcal{E}_{loc}(i) + \sum_{k \in \mathcal{P}, k \neq i} \mathcal{E}_{loc}(k) H(x_{ik}) \right), \quad (\text{A.25})$$

where $\mathcal{E}_{loc}(k) = (1 - \text{IoU}(k))/(1 - \tau)$. Here, we take $H(x)$ as a step function instead of its approximation for simplicity.

Table A.10 presents the computation of aLRP values including all by-products for each of the four positive anchors in $C\&R_1$, $C\&R_2$ and $C\&R_3$. Given the table presented in Figure 1(a) in the paper, we present how each column is derived in the following steps:

1. $1 - \text{IoU}(i)$ is simply the IoU Loss of the positive anchors after prediction.

Table A.10: Per-box calculation of \mathcal{L}_{aLRP}

Output	Anchor	$1 - \text{IoU}(i)$	$\mathcal{E}_{loc}(i)$	$\text{cumsum}(\mathcal{E}_{loc})(i)$	$N_{FP}(i)$	$\text{rank}(i)$	$\ell^{\text{LRP}}(i)$	$\mathcal{L}^{\text{aLRP}}$
C&R1	a_1	0.05	0.10	0.10	0.00	1.00	0.10	0.53
	a_3	0.20	0.40	0.50	1.00	3.00	0.50	
	a_6	0.35	0.70	1.20	3.00	6.00	0.70	
	a_{10}	0.50	1.00	2.20	6.00	10.00	0.82	
C&R2	a_1	0.20	0.40	0.40	0.00	1.00	0.40	0.69
	a_3	0.35	0.70	1.10	1.00	3.00	0.70	
	a_6	0.50	1.00	2.10	3.00	6.00	0.85	
	a_{10}	0.20	0.40	2.50	6.00	10.00	0.82	
C&R3	a_1	0.50	1.00	1.00	0.00	1.00	1.00	0.89
	a_3	0.35	0.70	1.70	1.00	3.00	0.90	
	a_6	0.20	0.40	2.10	3.00	6.00	0.85	
	a_{10}	0.05	0.10	2.20	6.00	10.00	0.82	

- $\mathcal{E}_{loc}(i) = (1 - \text{IoU}(i))/(1 - \tau)$ such that $\tau = 0.5$.
- Define a cumulative sum: $\text{cumsum}(\mathcal{E}_{loc})(i) = \mathcal{E}_{loc}(i) + \sum_{k \in \mathcal{P}, k \neq i} \mathcal{E}_{loc}(k)H(x_{ik})$ (see Eq. A.25). Note that this simply corresponds to a cumulative sum on a positive example using the examples with larger scores and itself. Accordingly, in Table A.10, $\text{cumsum}(\mathcal{E}_{loc})(i)$ is calculated by summing $\mathcal{E}_{loc}(i)$ column over anchors until (and including) i th example.
- $N_{FP}(i)$ is the number of negative examples with larger scores than the i th positive anchor. (See Section 3 for the formal definition.)
- $\text{rank}(i)$ is the rank of an example within positives and negatives. (See Section 2 for the formal definition.)
- Then using $\text{cumsum}(\mathcal{E}_{loc})(i)$, $N_{FP}(i)$ and $\text{rank}(i)$, LRP error on a positive example can be computed as:

$$\ell^{\text{LRP}}(i) = \frac{N_{FP}(i) + \text{cumsum}(\mathcal{E}_{loc})(i)}{\text{rank}(i)}. \quad (\text{A.26})$$

- In the rightmost column, aLRP Loss of a detector, $\mathcal{L}^{\text{aLRP}}$, is determined simply averaging over these single LRP values (i.e. $\ell^{\text{LRP}}(i)$) on positives.

B Details of Table 1: Hyperparameters of the Loss Functions and Models

This section presents the hyperparameters of the common loss functions in object detection and how they are combined by different models in Table 1.

B.1 Hyperparameters of the Individual Loss Functions

Table A.11 presents common loss functions and their hyperparameters. Note that since any change in these hyperparameter change the value of the loss function and affects its contribution to the multi-task learning nature of object detection, and, therefore w_r also needs to be retuned.

B.2 Hyperparameters of the Loss Functions of the Models

This section discusses the loss functions of the methods discussed in Table 1 in the paper. Obviously, AP Loss [7], Focal Loss [15] and DR Loss [26] follow the formulation in Equation 1. Hence using Table A.11, their total number of hyperparameters is easy to see. For example, DR Loss with three hyper-parameters is combined with Smooth L1, which has one hyperparameter. Including the weight of the localisation component, five hyper-parameters are required to be tuned.

Other architectures in Table 1 use more than two loss functions in order to learn different aspects to improve the performance:

Table A.11: Common loss functions and the hyperparameters in their definitions.

	Loss Function	Type	Number & Usage of the Hyper-parameters	
\mathcal{L}_c	Cross-entropy [17, 27]	Score-based	0	Sampling methods are required
	α -bal. Cross-entropy[15]	Score-based	1	The weight of the foreground anchors
	Focal Loss [15]	Score-based	2	The weight of the foreground anchors Modulating factor for hard examples
	AP Loss [7]	Ranking-based	1	Smoothness of the step function
	DR Loss [26]	Ranking-based	3	Regularizer for foreground distribution Regularizer for background distribution Smoothness of the loss
\mathcal{L}_r	Smooth L_1 [10]	l_p -based	1	Cut-off from L_1 loss to L_2 loss
	Balanced L_1 [23]	l_p -based	2	The weight of the inlier anchors Upper bound of the loss value
	IoU Loss [28]	IoU-based	0	-

- FCOS [30] includes an additional centerness branch to predict the centerness of the pixels, which is trained by an additional cross entropy loss.
- FreeAnchor [35] aims simultaneously to learn the assignment of the anchors to the ground truths by modeling the loss function based on maximum likelihood estimation. In Table 1, one can easily identify six hyper-parameters from the loss formulation of the Free Anchor and exploiting Table A.11. Moreover, the inputs of the focal loss are subject to a saturated linear function with two hyperparameters, which makes eight in total.
- A different set of approaches, an example of which is Faster R-CNN [27], uses directly cross entropy loss. However, cross entropy loss requires to be accompanied by a sampling method by which a set of positive and negative examples are sampled from the set of labelled anchors to alleviate the significant class imbalance. Even for random sampler, two of the following needs to be tuned in order to ensure stable training: (i) Number of positive examples (ii) Number of negative examples (iii) The rate between positives and negatives. Moreover, for a two-stage detector, these should be tuned for both stages, which brings about additional four hyper-parameters. That’s why Faster R-CNN [27] in Table 1 requires nine hyperparameters.
- Finally, CenterNet [8], as a state-of-the-art bottom-up method, has a loss function with several components while learning to predict the centers and the corners. It combines six individual losses, one of which is Hinge Loss with one hyperparameter. Considering the type of each, the loss function of CenterNet [8] has 10 hyper-parameters in total.

C Proofs of Theorem 1 and Theorem 2

This section presents the proofs for the theorems presented in our paper.

Theorem 1. $\mathcal{L} = \frac{1}{Z} \sum_{i \in \mathcal{P}} \ell(i) = \frac{1}{Z} \sum_{i \in \mathcal{P}} \sum_{j \in \mathcal{N}} L_{ij}$.

Proof. The ranking function is defined as:

$$\mathcal{L} = \frac{1}{Z} \sum_{i \in \mathcal{P}} \ell(i). \tag{A.27}$$

Since $\forall i \sum_{j \in \mathcal{N}} p(j|i) = 1$, we can rewrite the definition as follows:

$$\frac{1}{Z} \sum_{i \in \mathcal{P}} \ell(i) \left(\sum_{j \in \mathcal{N}} p(j|i) \right). \tag{A.28}$$

Reorganizing the terms concludes the proof as follows:

$$\frac{1}{Z} \sum_{i \in \mathcal{P}} \sum_{j \in \mathcal{N}} \ell(i)p(j|i) = \frac{1}{Z} \sum_{i \in \mathcal{P}} \sum_{j \in \mathcal{N}} L_{ij}. \tag{A.29}$$

□

Theorem 2. *Training is balanced between positive and negative examples at each iteration; i.e. the summed gradient magnitudes of positives and negatives are equal:*

$$\sum_{i \in \mathcal{P}} \left| \frac{\partial \mathcal{L}}{\partial s_i} \right| = \sum_{i \in \mathcal{N}} \left| \frac{\partial \mathcal{L}}{\partial s_i} \right|. \quad (\text{A.30})$$

Proof. The gradients of a ranking-based loss function are derived as (see Algorithm 1 and Equation 5 in the paper):

$$\frac{\partial \mathcal{L}}{\partial s_i} = \frac{1}{Z} \left(\sum_j \Delta x_{ij} - \sum_j \Delta x_{ji} \right) = \frac{1}{Z} \sum_j \Delta x_{ij} - \frac{1}{Z} \sum_j \Delta x_{ji}, \quad (\text{A.31})$$

such that Δx_{ij} is the update for x_{ij} s and defined as $\Delta x_{ij} = L_{ij}^* - L_{ij}$. Note that both L_{ij} and L_{ij}^* can be non-zero only if $i \in \mathcal{P}$ and $j \in \mathcal{N}$ following the definition of the primary term. Hence, the same applies to Δx_{ij} : if $i \notin \mathcal{P}$ or $j \notin \mathcal{N}$, then $\Delta x_{ij} = 0$. Then using these facts, we can state in Eq. (A.31) that if $i \in \mathcal{P}$, then $\sum_j \Delta x_{ji} = 0$; and if $i \in \mathcal{N}$, then $\sum_j \Delta x_{ij} = 0$. Then, we can say that, only one of the terms is active in Eq. (A.31) for positives and negatives:

$$\frac{\partial \mathcal{L}}{\partial s_i} = \underbrace{\frac{1}{Z} \sum_j \Delta x_{ij}}_{\text{Active if } i \in \mathcal{P}} - \underbrace{\frac{1}{Z} \sum_j \Delta x_{ji}}_{\text{Active if } i \in \mathcal{N}}. \quad (\text{A.32})$$

Considering that the value of a primary term cannot be less than its target, we have $\Delta x_{ij} \leq 0$, which implies $\frac{\partial \mathcal{L}}{\partial s_i} \leq 0$. So, we can take the absolute value outside of summation:

$$\sum_{i \in \mathcal{P}} \left| \frac{\partial \mathcal{L}}{\partial s_i} \right| = \left| \sum_{i \in \mathcal{P}} \frac{\partial \mathcal{L}}{\partial s_i} \right|, \quad (\text{A.33})$$

and using the fact identified in Eq. (A.32) (i.e. for $i \in \mathcal{P}$, $\frac{\partial \mathcal{L}}{\partial s_i} = \frac{1}{Z} \sum_{j \in \mathcal{N}} \Delta x_{ij}$):

$$\left| \sum_{i \in \mathcal{P}} \frac{1}{Z} \sum_{j \in \mathcal{N}} \Delta x_{ij} \right| = \left| \frac{1}{Z} \sum_{i \in \mathcal{P}} \sum_{j \in \mathcal{N}} \Delta x_{ij} \right|. \quad (\text{A.34})$$

Simply interchanging the indices and the order of summations, and then reorganizing the constant $\frac{1}{Z}$ respectively yields:

$$\left| \frac{1}{Z} \sum_{j \in \mathcal{P}} \sum_{i \in \mathcal{N}} \Delta x_{ji} \right| = \left| \frac{1}{Z} \sum_{i \in \mathcal{N}} \sum_{j \in \mathcal{P}} \Delta x_{ji} \right| = \left| \sum_{i \in \mathcal{N}} \frac{1}{Z} \sum_{j \in \mathcal{P}} \Delta x_{ji} \right|. \quad (\text{A.35})$$

Note that for $i \in \mathcal{N}$, $\frac{\partial \mathcal{L}}{\partial s_i} = -\frac{1}{Z} \sum_{j \in \mathcal{P}} \Delta x_{ji}$, and hence $\frac{1}{Z} \sum_{j \in \mathcal{P}} \Delta x_{ji} = -\frac{\partial \mathcal{L}}{\partial s_i}$. Replacing $\frac{1}{Z} \sum_{j \in \mathcal{P}} \Delta x_{ji}$:

$$\left| \sum_{i \in \mathcal{N}} -\frac{\partial \mathcal{L}}{\partial s_i} \right|. \quad (\text{A.36})$$

Since, for $i \in \mathcal{N}$, $\frac{\partial \mathcal{L}}{\partial s_i} = -\frac{1}{Z} \sum_{j \in \mathcal{P}} \Delta x_{ji}$ is greater or equal to zero, the proof follows:

$$\left| \sum_{i \in \mathcal{N}} -\frac{\partial \mathcal{L}}{\partial s_i} \right| = \left| \sum_{i \in \mathcal{N}} \frac{\partial \mathcal{L}}{\partial s_i} \right| = \sum_{i \in \mathcal{N}} \left| \frac{\partial \mathcal{L}}{\partial s_i} \right|. \quad (\text{A.37})$$

□

D Normalized Discounted Cumulative Gain (NDCG) Loss and Its Gradients: Another Case Example for our Generalized Framework

In the following we define and derive the gradients of the NDCG Loss [18] following our generalized framework presented in Section 3 of our main paper.

The NDCG loss is defined as:

$$\mathcal{L}^{\text{NDCG}} = 1 - \frac{1}{G_{max}} \sum_{i \in \mathcal{P}} G(i) = \frac{G_{max} - \sum_{i \in \mathcal{P}} G(i)}{G_{max}} = \sum_{i \in \mathcal{P}} \frac{G_{max}/|\mathcal{P}| - G(i)}{G_{max}}. \quad (\text{A.38})$$

Note that different from AP Loss and aLRP Loss, here Z turns out to be 1, which makes sense since NDCG is normalized by definition. Also, based on Eq. A.38, one can identify NDCG Error on a positive as: $\ell^{\text{NDCG}}(i) = \frac{G_{max}/|\mathcal{P}| - G(i)}{G_{max}}$ such that $G(i) = \frac{1}{\log_2(1+\text{rank}(i))}$ and $G_{max} = \sum_{i=1}^{|\mathcal{P}|} \log_2(1+i)$.

Similar to AP and aLRP Loss, using $p(j|i) = \frac{H(x_{ij})}{N_{FP}(i)}$, the primary term of the NDCG Loss is $L_{ij}^{\text{NDCG}} = \ell^{\text{NDCG}}(i)p(j|i)$ (line 1 of Algorithm 1 in the paper). When the positive example i is ranked properly, $G(i) = \frac{1}{\log_2(1+1)} = 1$, and resulting desired NDCG Error is (line 2 of Algorithm 1):

$$\ell^{\text{NDCG}}(i)^* = \frac{G_{max}/|\mathcal{P}| - 1}{G_{max}}, \quad (\text{A.39})$$

yielding a target primary term $L_{ij}^{\text{NDCG}*} = \ell_i^{\text{NDCG}*} p(j|i)$. Using L_{ij}^{NDCG} and $L_{ij}^{\text{NDCG}*}$, the update can be calculated as follows (line 3 of Algorithm 1):

$$\Delta x_{ij} = L_{ij}^{\text{NDCG}*} - L_{ij}^{\text{NDCG}} = \left(\ell^{\text{NDCG}}(i)^* - \ell^{\text{NDCG}}(i) \right) p(j|i), \quad (\text{A.40})$$

$$= \left(\frac{G_{max}/|\mathcal{P}| - G(i)}{G_{max}} - \frac{G_{max}/|\mathcal{P}| - 1}{G_{max}} \right) \frac{H(x_{ij})}{N_{FP}(i)}, \quad (\text{A.41})$$

$$= \frac{1 - G(i)}{G_{max}} \frac{H(x_{ij})}{N_{FP}(i)}, \quad (\text{A.42})$$

and one can compute the gradients using Eq. 5 in the paper (line 4 of Algorithm 1).

E Computing aLRP Loss and its Gradients

This section presents the algorithm to compute aLRP Loss in detail along with an analysis of space and time complexity. For better understanding, bold font denotes multi-dimensional data structures (which can be implemented by vectors, matrices or tensors). Algorithm A.2 describes the steps to compute aLRP Loss along with the gradients for a given mini-batch.

Description of the inputs: \mathbf{S} is the raw output of the classification branch, namely logits. For localisation, as done by IoU-based localisation losses [32, 28], the raw localisation outputs need to be converted to the boxes, which are denoted by \mathbf{B} . We assume that \mathbf{M} stores -1 for ignored anchors and 0 for negative anchors. For positive anchors, \mathbf{M} stores the index of the ground truth (i.e. $\{1, \dots, |\hat{\mathbf{B}}|\}$, where $\hat{\mathbf{B}}$ is a list of ground boxes for the mini-batch). Hence, we can find the corresponding ground truth for a positive anchor only by using \mathbf{M} . δ is the smoothness of the piecewise linear function defined in Eq. A.43 and set to 1 following AP Loss. We use the self-balance ratio, $\frac{\mathcal{L}^{\text{aLRP}}}{\mathcal{L}^{\text{cls}}}$, by averaging over its values from the previous epoch. We initialize it as 50 (i.e. see Table 4 in the paper).

Part 1: Initializing Variables: Lines 2-10 aim to initialize the necessary data from the inputs. While this part is obvious, please note that line 8 determines a threshold to select the relevant negative outputs. This is simply due to Eq. A.43 and the gradients of these negative examples with scores under this threshold are zero. Therefore, for the sake of time and space efficiency, they are ignored.

Part 2: Computing Unnormalized Localisation Errors: Lines 12-14 compute unnormalized localisation error on each positive example. Line 12 simply finds the localisation error of each positive example and line 13 sorts these errors with respect to their scores in descending order, and Line 14 computes the cumulative sum of the sorted errors with cumsum function. In such a way, the example with the larger scores contributes to the error computed for each positive anchor with smaller scores. Note that while computing the nominator of the \mathcal{L}_{loc}^{aLRP} , we employ the step function (not the piecewise linear function), since we can safely use backpropagation.

Part 3: Computing Gradient and Error Contribution from Each Positive: Lines 16-32 compute the gradient and error contribution from each positive example. To do so, Line 16 initializes necessary data structures. Among these data structures, while \mathcal{L}_{loc}^{LRP} , \mathcal{L}_{cls}^{LRP} and $\frac{\partial \mathcal{L}^{aLRP}}{\partial \mathbf{S}_+}$ are all with size $|\mathcal{P}|$, $\frac{\partial \mathcal{L}^{aLRP}}{\partial \mathbf{S}_-}$ has size $|\hat{\mathcal{N}}|$, where $\hat{\mathcal{N}}$ is the number of negative examples after ignoring the ones with scores less than τ in Line 8, and obviously $|\hat{\mathcal{N}}| \leq |\mathcal{N}|$. The loop iterates over each positive example by computing LRP values and gradients since aLRP is defined as the average LRP values over positives (see Eq. 9 in the paper). Lines 18-22 computes the relation between the corresponding positive with positives and relevant negatives, each of which requires the difference transformation followed by piecewise linear function:

$$H(x) = \begin{cases} 0, & x < -\delta \\ \frac{x}{2\delta} + 0.5, & -\delta \leq x \leq \delta \\ 1, & \delta < x. \end{cases} \quad (\text{A.43})$$

Then, using these relations, lines 23-25 compute the rank of the i th examples within positive examples, number of negative examples with larger scores (i.e. false positives) and rank of the example. Lines 26 and 27 compute aLRP classification and localisation errors on the corresponding positive example. Note that to have a consistent denominator for total aLRP, we use rank to normalize both of the components. Lines 28-30 compute the gradients. While the local error is enough to determine the unnormalized gradient of a positive example, the gradient of a negative example is accumulated through the loop.

Part 4: Computing aLRP Loss and Gradients: Lines 34-40 simply derive the final aLRP value by averaging over LRP values (lines 34-36), normalize the gradients (lines 37-38) and compute gradients wrt the boxes (line 39) and applies self balancing (line 40).

E.1 Time Complexity

- First 16 lines of Algorithm A.2 require time between $\mathcal{O}(|\mathcal{P}|)$ and $\mathcal{O}(|\mathcal{N}|)$. Since for the object detection problem, the number of negative examples is quite larger than number of positive anchors (i.e. $|\mathcal{P}| \ll |\mathcal{N}|$), we can conclude that the time complexity of first 13 lines is $\mathcal{O}(|\mathcal{N}|)$.
- The bottleneck of the algorithm is the loop on lines 17-32. The loop iterates over each positive example, and in each iteration while lines 21, 24 and 30 are executed for relevant negative examples, the rest of the lines is executed for positive examples. Hence the number of operations for each iteration is $\max(|\mathcal{P}|, |\hat{\mathcal{N}}|)$ (i.e. number of relevant negatives, see lines 8-9), and overall these lines require $\mathcal{O}(|\mathcal{P}| \times \max(|\mathcal{P}|, |\hat{\mathcal{N}}|))$. Note that, while in the early training epochs, $|\hat{\mathcal{N}}| \approx |\mathcal{N}|$, as the training proceeds, the classifier tends to distinguish positive examples from negative examples very well, and $|\hat{\mathcal{N}}|$ significantly decreases implying faster mini-batch iterations.
- The remaining lines between 26-33 again require time between $\mathcal{O}(|\mathcal{P}|)$ and $\mathcal{O}(|\mathcal{N}|)$.

Hence, we conclude that the time complexity of Algorithm A.2 is $\mathcal{O}(|\mathcal{N}| + |\mathcal{P}| \times \max(|\mathcal{P}|, |\hat{\mathcal{N}}|))$.

Compared to AP Loss;

- aLRP Loss includes an extra computation of aLRP localisation component (i.e. lines 12-14, 27. Each of these lines requires $\mathcal{O}(|\mathcal{P}|)$).
- aLRP Loss includes an additional summation while computing the gradients with respect to the scores of the positive examples in line 29 requiring $\mathcal{O}(|\mathcal{P}|^2)$.

- aLRP Loss discards interpolation (i.e. using interpolated AP curve), which can take up to $\mathcal{O}(|\mathcal{P}| \times |\hat{\mathcal{N}}|)$.

E.2 Space Complexity

Algorithm A.2 does not require any data structure larger than network outputs (i.e. \mathbf{B} , \mathbf{S}). Then, we can safely conclude that the space complexity is similar to all of the common loss functions that is $\mathcal{O}(|\mathbf{S}|)$.

F Details of aLRP Loss

This section provides details for aLRP Loss.

F.1 A Soft Sampling Perspective for aLRP Localisation Component

In sampling methods, the contribution (w_i) of the i th bounding box to the loss function is adjusted as follows:

$$\mathcal{L} = \sum_{i \in \mathcal{P} \cup \mathcal{N}} w_i \mathcal{L}(i), \quad (\text{A.44})$$

where $\mathcal{L}(i)$ is the loss of the i th example. Hard and soft sampling approaches differ on the possible values of w_i . For the hard sampling approaches, $w_i \in \{0, 1\}$, thus a BB is either selected or discarded. For soft sampling approaches, $w_i \in [0, 1]$, i.e. the contribution of a sample is adjusted with a weight and each BB is somehow included in training. While this perspective is quite common to train the classification branch [3, 15]; the localisation branch is conventionally trained by hard sampling with some exceptions (e.g. CARL [3] sets $w_i = s_i$ where s_i is the classification score).

Here, we show that, in fact, what aLRP localisation component does is soft sampling. To see this, first let us recall the definition of the localisation component:

$$\mathcal{L}_{loc}^{\text{aLRP}} = \frac{1}{|\mathcal{P}|} \sum_{i \in \mathcal{P}} \frac{1}{\text{rank}(i)} \left(\mathcal{E}_{loc}(i) + \sum_{k \in \mathcal{P}, k \neq i} \mathcal{E}_{loc}(k) H(x_{ik}) \right), \quad (\text{A.45})$$

which is differentiable with respect to the box parameters as discussed in the paper. With a ranking-based formulation, note that (i) the localisation error of a positive example i (i.e. $\mathcal{E}_{loc}(i)$) contributes each LRP value computed on a positive example j where $s_i \geq s_j$ (also see Fig. 2 in the paper), and (ii) each LRP value computed on a positive example i is normalized by $\text{rank}(i)$. Then, setting $\mathcal{L}(i) = \mathcal{E}_{loc}(i)$ in Eq. A.44 and accordingly taking Eq. A.45 in $\mathcal{E}_{loc}(i)$ paranthesis, the weights of the positive examples (i.e. $w_i = 0$ for negatives for the localisation component) are:

$$w_i = \frac{1}{|\mathcal{P}|} \left(\left(\sum_{k \in \mathcal{P}, k \neq i} \frac{H(x_{ki})}{\text{rank}(k)} \right) + \frac{1}{\text{rank}(i)} \right). \quad (\text{A.46})$$

Note that $\mathcal{L}(i)$ is based on a differentiable IoU-based regression loss and w_i is its weight, which is a scalar. As a result $H(x_{ki})$ in Eq. A.46 does not need to be smoothed and we use a unit-step function (see line 14 in Algorithm A.2).

F.2 The Relation between aLRP Loss Value and Total Gradient Magnitudes

Here, we identify the relation between the loss value and the total magnitudes of the gradients following the generalized framework due to the fact that it is a basis for our self-balancing strategy introduced in Section 4.2 as follows:

$$\sum_{i \in \mathcal{P}} \left| \frac{\partial \mathcal{L}}{\partial s_i} \right| = \sum_{i \in \mathcal{N}} \left| \frac{\partial \mathcal{L}}{\partial s_i} \right| \approx \mathcal{L}^{\text{aLRP}}. \quad (\text{A.47})$$

Algorithm A.2 The algorithm to compute aLRP Loss for a mini-batch.

Input: **S**: Logit predictions of the classifier for each anchor,
B: Box predictions of the localization branch from each anchor,
 $\hat{\mathbf{B}}$: Ground truth (GT) boxes,
M: Matching of the anchors with the GT boxes.
 δ : Smoothness of the piece-wise linear function ($\delta = 1$ by default).
 w_{ASB} : ASB weight, computed using $\frac{\mathcal{L}^{aLRP}}{\mathcal{L}^{cls}}$ values from previous epoch.

Output: \mathcal{L}^{aLRP} : aLRP loss, $\frac{\partial \mathcal{L}^{aLRP}}{\partial \mathbf{S}}$: Gradients wrt logits, $\frac{\partial \mathcal{L}^{aLRP}}{\partial \mathbf{B}}$: Gradients wrt boxes.

```

1: // Part 1: Initializing Variables
2:  $\mathbf{idx}_+$  := The indices of M where  $\mathbf{M} > 0$ .
3:  $\mathbf{M}_+$  := The values of M where  $\mathbf{M} > 0$ .
4:  $\mathbf{B}_+$  := The values of B at indices  $\mathbf{idx}_+$ .
5:  $\mathbf{S}_+$  := The values of S at indices  $\mathbf{idx}_+$ .
6:  $\mathbf{idx}_+^{\text{sorted}}$  := The indices of  $\mathbf{S}_+$  once it is sorted in descending order.
7:  $\mathbf{S}_+^{\text{sorted}}$  := The values of  $\mathbf{S}_+$  when ordered according to  $\mathbf{idx}_+^{\text{sorted}}$ .
8:  $\tau = \min(\mathbf{S}_+) - \delta$ .
9:  $\mathbf{idx}_-$  := The indices of M where  $\mathbf{M} = 0$  and  $s_j \geq \tau$  (i.e. relevant negatives only).
10:  $\mathbf{S}_-$  := The values of S at indices  $\mathbf{idx}_-$ .
11: // Part 2: Computing Unnormalized Localisation Errors
12:  $\mathcal{E}_{\text{Loc}} = \frac{1 - \text{IoU}(\mathbf{B}_+, \hat{\mathbf{B}}_+)}{1 - \tau}$ . (or  $\mathcal{E}_{\text{Loc}} = \frac{(1 - \text{GIoU}(\mathbf{B}_+, \hat{\mathbf{B}}_+))/2}{1 - \tau}$  for GIoU Loss [28].)
13:  $\mathcal{E}_{\text{Loc}}^{\text{sorted}}$  := The values of  $\mathcal{E}_{\text{Loc}}$  when ordered according to  $\mathbf{idx}_+^{\text{sorted}}$ .
14:  $\mathcal{E}_{\text{Loc}}^{\text{cumsum}} = \text{cumsum}(\mathcal{E}_{\text{Loc}}^{\text{sorted}})$ 
15: // Part 3: Computing Gradient and Error Contribution from Each Positive
16: Initialize  $\mathcal{L}_{\text{loc}}^{\text{LRP}}$ ,  $\mathcal{L}_{\text{cls}}^{\text{LRP}}$ ,  $\frac{\partial \mathcal{L}^{aLRP}}{\partial \mathbf{S}_+}$  and  $\frac{\partial \mathcal{L}^{aLRP}}{\partial \mathbf{S}_-}$ .
17: for each  $s_i \in \mathbf{S}_+^{\text{sorted}}$  do
18:    $\mathbf{X}_+$  := Difference transform of  $s_i$  with the logit of each positive example.
19:    $\mathbf{R}_+$  := The relation of  $i \in \mathcal{P}$  with each  $j \in \mathcal{P}$  using Eq. A.43 with input  $\mathbf{X}_+$ .
20:    $\mathbf{R}_+[i] = 0$ 
21:    $\mathbf{X}_-$  := Difference transform of  $s_i$  with the logit of each negative example.
22:    $\mathbf{R}_-$  := The relation of  $i \in \mathcal{P}$  with each  $j \in \mathcal{N}$  using Eq. A.43 with input  $\mathbf{X}_+$ .
23:    $\text{rank}_+ = 1 + \text{sum}(\mathbf{R}_+)$ 
24:    $\text{FP} = \text{sum}(\mathbf{R}_-)$ 
25:    $\text{rank} = \text{rank}_+ + \text{FP}$ 
26:    $\mathcal{L}_{\text{cls}}^{\text{LRP}}[i] = \text{FP} / \text{rank}$ 
27:    $\mathcal{L}_{\text{loc}}^{\text{LRP}}[i] = \mathcal{E}_{\text{Loc}}^{\text{cumsum}}[i] / \text{rank}$ 
28:   if  $\text{FP} \geq \epsilon$  then //For stability set  $\epsilon$  to a small value (e.g.  $1e - 5$ )
29:      $\frac{\partial \mathcal{L}^{aLRP}}{\partial \mathbf{S}_+}[i] = - \left( \text{FP} + \sum_{i \in \mathcal{P}} \mathbf{R}_+[i] \times \mathcal{E}_{\text{Loc}}^{\text{cumsum}}[i] \right) / \text{rank}$ 
30:      $\frac{\partial \mathcal{L}^{aLRP}}{\partial \mathbf{S}_-} += \left( - \frac{\partial \mathcal{L}^{aLRP}}{\partial \mathbf{S}_+}[i] \times \frac{\mathbf{R}_-}{\text{FP}} \right)$ 
31:   end if
32: end for
33: // Part 4: Computing the aLRP Loss and Gradients
34:  $\mathcal{L}_{\text{cls}}^{\text{aLRP}} = \text{mean}(\mathcal{L}_{\text{cls}}^{\text{LRP}})$ 
35:  $\mathcal{L}_{\text{loc}}^{\text{aLRP}} = \text{mean}(\mathcal{L}_{\text{loc}}^{\text{LRP}})$ 
36:  $\mathcal{L}^{\text{aLRP}} = \mathcal{L}_{\text{cls}}^{\text{aLRP}} + \mathcal{L}_{\text{loc}}^{\text{aLRP}}$ 
37: Place  $\frac{\partial \mathcal{L}^{\text{aLRP}}}{\partial \mathbf{S}_+}$  and  $\frac{\partial \mathcal{L}^{\text{aLRP}}}{\partial \mathbf{S}_-}$  into  $\frac{\partial \mathcal{L}^{\text{aLRP}}}{\partial \mathbf{S}}$  also by setting the gradients of remaining examples to 0.
38:  $\frac{\partial \mathcal{L}^{\text{aLRP}}}{\partial \mathbf{S}} / = |\mathcal{P}|$ 
39: Compute  $\frac{\partial \mathcal{L}^{\text{aLRP}}}{\partial \mathbf{B}}$  (possibly using autograd property of a deep learning library or refer to the supp. mat. of [28] for the gradients of GIoU and IoU Losses.
40:  $\frac{\partial \mathcal{L}_{\text{loc}}^{\text{aLRP}}}{\partial \mathbf{B}} \times = w_{ASB}$ 
41: return  $\frac{\partial \mathcal{L}^{\text{aLRP}}}{\partial \mathbf{S}}$ ,  $\frac{\partial \mathcal{L}^{\text{aLRP}}}{\partial \mathbf{B}}$  and  $\mathcal{L}^{\text{aLRP}}$ .

```

Since we showed in Section C that $\sum_{i \in \mathcal{P}} \left| \frac{\partial \mathcal{L}}{\partial s_i} \right| = \sum_{i \in \mathcal{N}} \left| \frac{\partial \mathcal{L}}{\partial s_i} \right|$, here we show that the loss value is approximated by the total magnitude of gradients. Recall from Eq. (A.34) that total gradients of the positives can be expressed as:

$$\sum_{i \in \mathcal{P}} \left| \frac{\partial \mathcal{L}}{\partial s_i} \right| = \left| \frac{1}{|\mathcal{P}|} \sum_{i \in \mathcal{P}} \sum_{j \in \mathcal{N}} \Delta x_{ij} \right|. \quad (\text{A.48})$$

Since $\Delta x_{ij} \leq 0$, we can discard the absolute value by multiplying it by -1 :

$$-\frac{1}{|\mathcal{P}|} \sum_{i \in \mathcal{P}} \sum_{j \in \mathcal{N}} \Delta x_{ij}. \quad (\text{A.49})$$

Replacing the definition of the Δx_{ij} by $L_{ij}^* - L_{ij}$ yields:

$$-\frac{1}{|\mathcal{P}|} \sum_{i \in \mathcal{P}} \sum_{j \in \mathcal{N}} (L_{ij}^* - L_{ij}) = -\frac{1}{|\mathcal{P}|} \left(\sum_{i \in \mathcal{P}} \sum_{j \in \mathcal{N}} L_{ij}^* - \sum_{i \in \mathcal{P}} \sum_{j \in \mathcal{N}} L_{ij} \right) \quad (\text{A.50})$$

$$= \frac{1}{|\mathcal{P}|} \sum_{i \in \mathcal{P}} \sum_{j \in \mathcal{N}} L_{ij} - \frac{1}{|\mathcal{P}|} \sum_{i \in \mathcal{P}} \sum_{j \in \mathcal{N}} L_{ij}^*. \quad (\text{A.51})$$

Using Theorem 1, the first part (i.e. $\frac{1}{|\mathcal{P}|} \sum_{i \in \mathcal{P}} \sum_{j \in \mathcal{N}} L_{ij}$) yields the loss value, \mathcal{L} . Hence:

$$\sum_{i \in \mathcal{P}} \left| \frac{\partial \mathcal{L}}{\partial s_i} \right| = \mathcal{L} - \frac{1}{|\mathcal{P}|} \sum_{i \in \mathcal{P}} \sum_{j \in \mathcal{N}} L_{ij}^*. \quad (\text{A.52})$$

Reorganizing the terms, the difference between the total gradients of positives (or negatives, since they are equal – see Theorem 2) and the loss values itself is the sum of the targets normalized by number of positives:

$$\mathcal{L} - \sum_{i \in \mathcal{P}} \left| \frac{\partial \mathcal{L}}{\partial s_i} \right| = \frac{1}{|\mathcal{P}|} \sum_{i \in \mathcal{P}} \sum_{j \in \mathcal{N}} L_{ij}^*. \quad (\text{A.53})$$

Compared to the primary terms, the targets are very small values (if not 0). For example, for AP Loss $L_{ij}^{\text{AP}^*} = 0$, and hence, loss is equal to the sum of the gradients: $\mathcal{L} = \sum_{i \in \mathcal{P}} \left| \frac{\partial \mathcal{L}}{\partial s_i} \right|$.

As for aLRP Loss, the target of a primary term is $\frac{\mathcal{E}_{loc}(i)}{\text{rank}(i)} \frac{H(x_{ij})}{N_{FP}(i)}$, hence if $H(x_{ij}) = 0$, then the target is also 0. Else if $H(x_{ij}) = 1$, then it implies that there are some negative examples with larger scores, and $\text{rank}(i)$ and $N_{FP}(i)$ are getting larger depending on these number of negative examples, which causes the denominator to grow, and hence yielding a small target as well. Then ignoring this term, we conclude that:

$$\sum_{i \in \mathcal{P}} \left| \frac{\partial \mathcal{L}}{\partial s_i} \right| = \sum_{i \in \mathcal{N}} \left| \frac{\partial \mathcal{L}}{\partial s_i} \right| \approx \mathcal{L}^{\text{aLRP}}. \quad (\text{A.54})$$

F.3 Self-balancing the Gradients Instead of the Loss Value

Instead of localisation the loss, $\mathcal{L}_{loc}^{\text{aLRP}}$, we multiply $\partial \mathcal{L} / \partial B$ by the average $\mathcal{L}^{\text{aLRP}} / \mathcal{L}_{loc}^{\text{aLRP}}$ of the previous epoch. This is because formulating aLRP Loss as $\mathcal{L}_{loc}^{\text{aLRP}} + w_r \mathcal{L}_{loc}^{\text{aLRP}}$ where w_r is a weight to balance the tasks is different from weighing the gradients with respect to the localisation output, B , since weighing the loss value (i.e. $\mathcal{L}_{loc}^{\text{aLRP}} + w_r \mathcal{L}_{loc}^{\text{aLRP}}$) changes the gradients of aLRP Loss with respect to the classification output as well since $\mathcal{L}_{loc}^{\text{aLRP}}$, now weighed by w_r , is also ranking-based (has $\text{rank}(i)$ term - see Eq. 11 in the paper). Therefore, we directly add the self balance term as a multiplier of $\partial \mathcal{L} / \partial B$ and backpropagate accordingly. On the other hand, from a practical perspective, this can simply be implemented by weighing the loss value, $\mathcal{L}_{loc}^{\text{aLRP}}$ without modifying the gradient formulation for $\mathcal{L}_{cls}^{\text{aLRP}}$.

Table A.12: Using Self Balance and GIoU with AP Loss. For optimal LRP (oLRP), lower is better.

\mathcal{L}_c	\mathcal{L}_r	SB	AP	AP ₅₀	AP ₇₅	AP ₉₀	oLRP	ρ
AP Loss [7]	Smooth L1		35.5	58.0	37.0	9.0	71.0	0.45
	Smooth L1	✓	36.7	58.2	39.0	10.8	70.2	0.44
	IoU Loss		36.3	57.9	37.9	11.8	70.4	0.44
	IoU Loss	✓	37.2	58.1	39.2	13.1	69.6	0.44
	GIoU Loss		36.5	58.1	38.1	11.9	70.2	0.45
	GIoU Loss	✓	37.2	58.3	39.0	13.4	69.7	0.44
aLRP Loss	with IoU		36.9	57.7	38.4	13.9	69.9	0.49
	with IoU	✓	38.7	58.1	40.6	17.4	68.5	0.48
	with GIoU	✓	38.9	58.5	40.5	17.4	68.4	0.48

G Additional Experiments

This section presents more ablation experiments, the anchor configuration we use in our models and the effect of using a wrong target for the primary term in the error-driven update rule.

G.1 More Ablation Experiments: Using Self Balance and GIoU with AP Loss

We also test the effect of GIoU and our Self-balance approach on AP Loss, and present the results in Table A.12:

- Using IoU-based losses with AP Loss improves the performance up to 1.0 AP as well and reaches 36.5 AP with GIoU loss.
- Our SB approach also improves AP Loss between 0.7 - 1.2 AP, resulting in 37.2AP as the best performing model without using w_r . However, it may not be inferred that SB performs better than constant weighting for AP Loss without a more thorough tuning of AP Loss since SB is devised to balance the gradients of localisation and classification outputs for aLRP Loss (see Section F.2).
- Comparing with the best performing model of AP Loss with 37.2AP, (i) aLRP Loss has a 1.7AP and 1.3oLRP points better performance, (ii) the gap is 4.0AP for AP₉₀, and (iii) the correlation coefficient of aLRP Loss, preserves the same gap (0.48 vs 0.44 comparing the best models for AP and aLRP Losses), since applying these improvements (IoU-based losses and SB) to AP Loss does not have an effect on unifying branches.

G.2 Anchor Configuration

The number of anchors has a notable affect on the efficiency of training due to the time and space complexity of optimizing ranking-based loss functions by combining error-driven update and back-propagation. For this reason, different from original RetinaNet using three aspect ratios (i.e. $[0.5, 1, 2]$) and three scales (i.e. $[2^{0/2}, 2^{1/2}, 2^{2/2}]$) on each location, Chen et al. [7] preferred the same three aspect ratios, but reduced the scales to two as $[2^{0/2}, 2^{1/2}]$ to increase the efficiency of AP Loss. In our ablation experiments, except the one that we used ATSS [34], we also followed the same anchor configuration of Chen et al. [7].

One main contribution of ATSS is to simplify the anchor design by reducing the number of required anchors to a single scale and aspect ratio (i.e. ATSS uses 1/9 and 1/6 of the anchors of RetinaNet [15] and AP Loss [7] respectively), which is a perfect fit for our optimization strategy. For this reason, we used ATSS, however, we observed that the configuration in the original ATSS with a single aspect ratio and scale does not yield the best result for aLRP Loss, which may be related to the ranking nature of aLRP Loss which favors more examples to impose a more accurate ranking, loss and gradient computation. Therefore, different from ATSS configuration, we find it useful to set anchor scales $[2^{0/2}, 2^{1/2}]$ and $[2^{0/2}, 2^{1/2}, 2^{2/2}]$ for aLRPLoss500 and aLRPLoss800 respectively and use a single aspect ratio with 1 following the original design of ATSS.

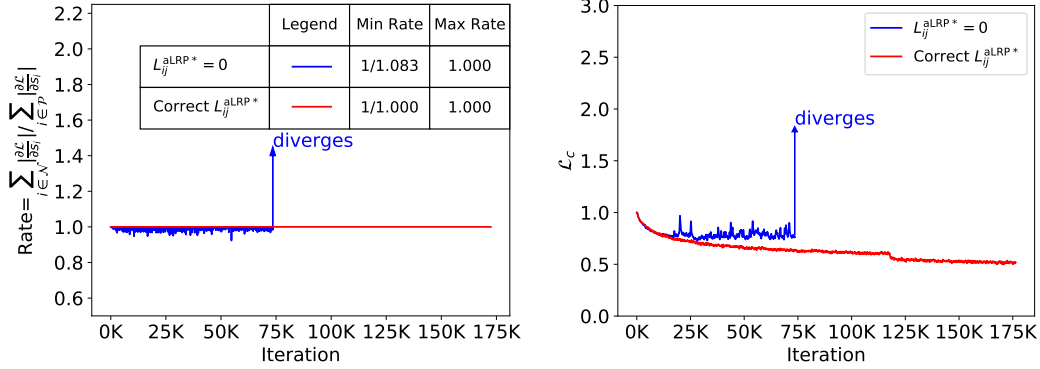


Figure A.7: (left) The rate of the total gradient magnitudes of negatives to positives. (right) Loss values.

G.3 Using a Wrong Target for the Primary Term in the Error-driven Update Rule

As discussed in our paper (Section 4.1, Equation 13), L_{ij}^* , the target value of the primary term L_{ij} is non-zero due to the localisation error. It is easy to overlook this fact and assume that the target is zero. Fig. A.7 presents this case where L_{ij}^* is set to 0 (i.e. minimum value of aLRP). In such a case, the training continues properly, similar to that of the correct case, up to a point and then diverges. Note that this occurs when the positives start to be ranked properly but are still assigned gradients since $L_{ij}^* - L_{ij} \neq 0$ due to the nonzero localisation error. This causes $\sum_{i \in \mathcal{P}} \left| \frac{\partial \mathcal{L}}{\partial s_i} \right| > \sum_{i \in \mathcal{N}} \left| \frac{\partial \mathcal{L}}{\partial s_i} \right|$, violating Theorem 2 (compare min-rate and max-rate in Fig. A.7). Therefore, assigning proper targets as indicated in Section 3 in the paper is crucial for balanced training.

G.4 Implementation Details for FoveaBox and Faster R-CNN

In this section, we provide more implementation details on the FoveaBox and Faster R-CNN models that we trained with different loss functions. All the models in this section are tested on COCO *minival*.

Implementation Details of FoveaBox: We train the models for 100 epochs with a learning rate decay at epochs 75 and 95. For aLRP Loss and AP Loss, we preserve the same learning rates used for RetinaNet (i.e. 0.008 and 0.002 for aLRP Loss and AP Loss respectively). As for the Focal Loss, we set the initial learning rate to 0.02 following the linear scheduling hypothesis [24] (i.e. Kong et al. set learning rate to 0.01 and use a batch size of 16). Following AP Loss official implementation, the gradients of the regression loss (i.e. Smooth L1) are averaged over the output parameters of positive boxes for AP Loss. As for Focal Loss, we follow the mmdetection implementation which averages the total regression loss by the number of positive examples. The models are tested on COCO *minival* by preserving the standard design by mmdetection framework.

Implementation Details of Faster R-CNN: To train Faster R-CNN, we first replace the softmax classifier of Fast R-CNN by the class-wise sigmoid classifiers. Instead of heuristic sampling rules, we use all anchors to train RPN and top-1000 scoring proposals per image obtained from RPN to train Fast R-CNN (i.e. same with the default training except for discarding sampling). Note that, with aLRP Loss, the loss function consists of two independent losses instead of four in the original pipeline, hence instead of three scalar weights, aLRP Loss requires a single weight for RPN head, which we tuned as 0.20. Following the positive-negative assignment rule of RPN, different from all the experiments, which use $\tau = 0.50$, $\tau = 0.70$ for aLRP Loss of RPN. We set the initial learning rate to 0.04 following the linear scheduling hypothesis [24] for the baselines, and decreased by a factor of 0.10 at epochs 75 and 95. Localisation loss weight is kept as 1 for L1 Loss and to 10 for GIoU Loss [6, 28]. The models are tested on COCO *minival* by preserving the standard design by mmdetection framework. We do not train Faster R-CNN with AP Loss due to the difficulty to tune Faster R-CNN for a different loss function.